A VEHICLE-TO-INFRASTRUCTURE BASED DYNAMIC MERGE ASSISTANCE

METHOD FOR MIXED TRAFFIC WITH MANUAL VEHICLE, CONNECTED

VEHICLE, AND AUTOMATED VEHICLES IN HIGHWAY MERGING SECTION

By

XIAOWEN JIANG

A dissertation submitted to the

School of Graduate Studies

Rutgers, The State University of New Jersey

In partial fulfillment of the requirements

For the degree of Doctor of Philosophy

Graduate Program in Civil and Environmental Engineering

Written under the direction of

Peter J. Jin

And approved by

_____

_____

_____

_____

New Brunswick, New Jersey

May, 2019

ABSTRACT OF THE DISSERTATION

A Vehicle-to-Infrastructure based Dynamic Merge Assistance Method for Mixed Traffic with Manual Vehicle, Connected Vehicle, and Automated Vehicles in Highway Merging Section

By XIAOWEN JIANG

Dissertation Director:

Peter J. Jin

Merging activities on the highway can cause significant recurrent and non-recurrent bottleneck congestion and is a severe issue in traffic operations. The efficient enhancement of highway merging activities has been considered as a major task in highway management research and practice. Some macroscopic active traffic management (ATM) methods have been proposed to mitigate bottleneck congestion. In recent years, microscopic dynamic merging assistance (DMA) methods have been proposed as efficient methods to improve the mobility and safety in merging maneuver. These proposed methods have been serving their roles as effective merge control methods for decades. Despite some positive outcomes of these existing methods in the improvement of the highway merge traffic, there are still some gaps for new merge assistance methods to catch. Recent developments and deployments of Automated Vehicle (AV) technologies and Connected Vehicle (CV) technologies such as Vehicle-to-Vehicle (V2V) and Vehicle-to-Infrastructure (V2I)

communication provide new opportunities for developing more efficient merge assistance methods. This leads the new wave of Connected-Automated-Vehicle (CAV) based DMA methods.

This dissertation proposes a microscopic CAV V2I-based Dynamic Merge Assistance (DMA) method for mixed types of vehicles including manual vehicle (MV), manually controlled connected vehicle (CV) and connected automated vehicle (CAV). The research starts from a comprehensive review of existing merge assistance methods and the evolution of microscopic DMA mechanisms and algorithms. Then integrated partial coordination merging control algorithm based on a pairing between mainline gaps and on-ramp merging vehicles (vehicle-gap pair) is proposed. The vehicle-gap pair is determined by a prediction of their merging potential, and the merging potential is predicted according to their instantaneous virtual trajectories (IVT) which are generated from the instantaneous lane speed profiles (ISP) of both mainline and onramp which consists of all detected vehicles' location and speed at each time frame. The pairing scenario varies with different combinations of vehicle types (i.e., MV, CV, CAV) involved in a merging maneuver. These scenarios involve vehicles with different features in terms of control, sensing, and communication. Thus, a set of 4-level pairing criteria is proposed to fit the DMA method in the universal traffic environment with mixed vehicle types. The pairing process is then followed by a coordination car-following control specifically designed for different vehicle types. The coordination car-following control maintains the mainline gaps for the paired on-ramp vehicle and guarantees the on-ramp vehicle can catch up with the paired gap safely and smoothly. Different control mechanisms are proposed based on the observability,

controllability, and the availability of communication in different vehicle combinations which is aligned to the 4-level pairing scenarios.

A VISSIM simulation is built based on the traffic flow data collected from the I-35 corridor in Austin TX with multiple merging and weaving sections. The proposed DMA model is implemented through a VISSIM Application Programming Interface (API) named external drivers' model (ETM). The safety performance of merging is evaluated by time-to-collision (TTC) and critical gap size (gap between mainline following vehicle and lane-changing on-ramp vehicle). The mobility performance is evaluated by average travel time and speed contour map in the whole simulation area including on-ramp, mainline merging area and mainline upstream. The proposed method is found to have a promising performance in both mobility and safety impact, especially on the on-ramp traffic during peak hours.

ACKNOWLEDGMENTS

I am so grateful that I can present this long-term research in the dissertation. I hope it can be a memorable gift for my student career, and if only it could bring even a little inspiration to the following researches.

Table of Contents

LIST OF TABLES

LIST OF FIGURES

1   Introduction

Along with the city expanding and population growing, the increasingly heavy traffic demand brings to the traffic system a more and more critical challenge in congestion and incidents on highways and urban corridors. One of the most severe issues is conflicts among merging vehicles near highway on-ramp and weaving areas which can lead to significant traffic bottlenecks. According to the congestion database reported by Texas A&M Transportation Institute (TAMU-TTI, 2015), the major urban areas in the U.S. are suffering from heavy highway mobility problems. The average yearly delay per auto commuter in 15 vast areas (e.g., DC-VA-MD Area, NY-NJ-CT Area, etc.) is 63 hours while excess fuel per auto commuter is 27 gallons and congestion cost per auto commuter is 1433 U.S. Dollars. The numbers of 31 large area (e.g., San Jose, Austin, etc.) are respectively 45 hours, 21 gallons, and 1045 dollars. It's difficult to count how much merging maneuver contributes to the congestion precisely. However, a report for U.S. Federal Highway Administration ("Traffic Congestion and Reliability: Trends and Advanced Strategies for Congestion Mitigation," 2005) claims that merging maneuver occurring in highway weaving and on-ramp section is one of seven sources of highway congestion, and the merging maneuver will cause the most severe impact on traffic flow. As a result, efficient enhancement of highway merging activities has been considered as a major task in highway management research and practice.
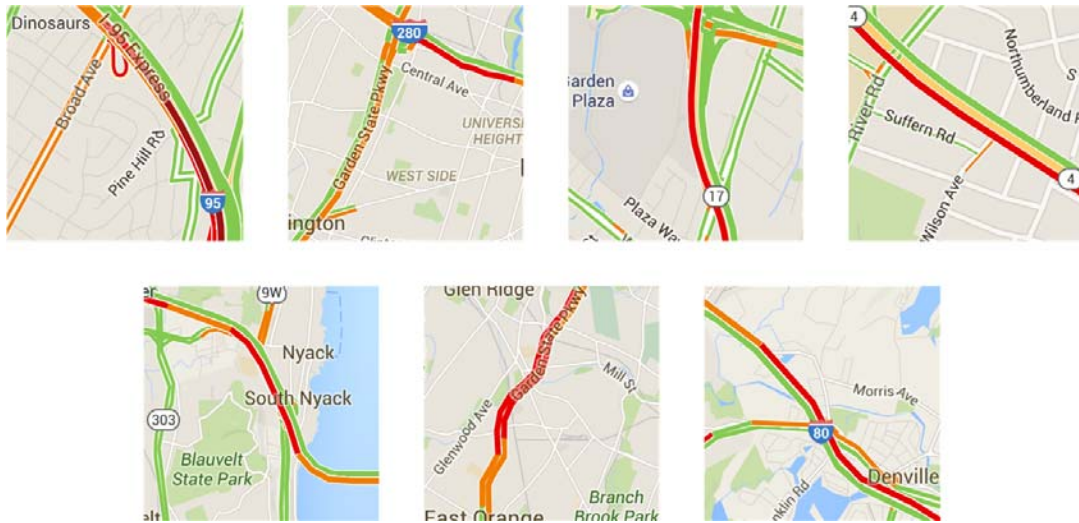
Figure 1 Typical Traffic on the Most Congested Corridors Segments in NJ

(figures are from Google Map)

Merge assistance methods are proposed and applied to improve merging performance. Some macroscopic Active Traffic Management (ATM) strategies including ramp metering (RM), queue warning system (QWS), variable speed limit (VSL), dynamic lane control (DLC), and Dynamic Merge Control have been proposed. These popular macroscopic ATM methods have different features to mitigate merging bottlenecks. RM and DLC control the on-ramp flow/capacity to guarantee the mainline (target-lane) mobility. QWS, VSL control the traffic speed to guarantee safer merging. Dynamic Merge Control is a density/gap control method including Early Merge, Late Merge, Dynamic Merge, Dynamic Lane Control, and Gap Metering (GM).

Along with the development of Intelligent Transportation System (ITS) technologies, some microscopic methods including Adaptive Cruise Control/Cooperative Adaptive Cruise Control (ACC/CACC)-based methods and some intelligent Dynamic Merging Assistance (DMA) methods are proposed by researchers. The representative

models include Automated Highway System (AHS)-based accurate vehicle control methods and autonomous vehicle control methods (e.g., automated-vehicle, Adaptive Cruise Control (ACC)/Cooperative Adaptive Cruise Control (CACC)).

Although these merge assistance methods have been brought into researches and practices for decades, and some positive outcomes have proved their abilities in the improvement of the highway merge traffic, there are still some gaps for new merge assistance methods to catch. The representative macroscopic methods encounter the control limitations due to the needs of additional particular roadside sign and signal systems and the issues on ensuring driver compliance. Meanwhile, these methods' single-scenario-aimed features limit their system flexibility. Most microscopic DMA methods also rely on highly-connected or automated traffic environment to achieve optimal performance and are restricted by the availability of vehicular technologies in the prevailing transportation systems. Recently, the accelerated development and deployment of the connected vehicle (CV) technologies and Automated Vehicle (AV) technologies, as well as Connected Automated Vehicle (CAV) technologies, provides new opportunities for developing more efficient merge assistance methods. This has made the Connected-Automated-Vehicle (CAV) based DMA method a hot topic in recent years.

1.1 Problem Statement

The merging activities usually can be considered as a process of two-lane traffic merging into the same lane which causes a significant capacity-drop. Besides the conflicts of normal lane-changing behavior, the conflicts between two traffic flow coupled with the capacity-drop during the merging process lead to more severe delays on both lanes. Furthermore, compared with a general "lane-drop" issue on arterial, the merging activity in highway

merging and weaving section has some different features. Firstly, the two traffics, noted mainline traffic and on-ramp traffic, usually have a significant speed difference. The faster traffic will be disrupted more and suffer from a heavier delay, while the slower one will take the higher cost to wait for merging. Besides the mobility impact, the significant speed difference will also lead to higher safety risk due to the remarkable speed oscillation during the acceleration/deceleration process. Secondly, the mainline traffic and on-ramp traffic has different priorities in right of way. Mainline traffic naturally has a higher priority in practice. It may cause the on-ramp traffic to bear a higher risk for an excellent opportunity to accelerate and catch up with relatively small mainline gaps. On the other hand, it may also force the faster on-ramp traffic to slow down and wait longer to merge to congested mainline traffic. In sum, highway on-ramp/weaving merging traffic will provide less and insufficient gaps compared with normal 2-to-1 lane-drop, and the system efficiency and safety will have a more remarkable decrease.

Since this is a common concern in highway traffic management, the topic on how to improve merging performance has been discussed for decades. Some microscopic merge assistance methods controlled the on-ramp traffic (e.g., the entry of on-ramp vehicles) to fit merging vehicles into mainline gaps. A significant benefit is these methods can protect mainline efficiency and safety by the compliance of on-ramp vehicles to the control signals. However, the on-ramp vehicles may suffer from even heavier queueing and congestion, especially in the condition of high merging demand. Meanwhile, some proposed methods which control mainline traffic to collect up the scattered gaps to a larger one for the on-ramp merging vehicles also have its pros and cons. These methods can mitigate on-ramp congestion effectively. However, they usually influence the mainline

traffic's efficiency and safety. Thus, the DMA methods which consider both on-ramp and mainline vehicles to implement a coordinated merging control are a better choice for researchers. Although a large part of the next proposed DMA methods also only control one side of traffic (i.e., either on-ramp or mainline), they utilize the information from another side indeed.

These coordinated merging assistance methods employ an automated highway system (AHS) or connected vehicle (CV) technologies to achieve the awareness of system-wide traffic information. They usually also lead a better delivery of control signals directed towards the drivers or vehicle controllers. Some low-automation-scale control methods send advisory signals to drivers who may be compliant, while some high-automation-scale methods implement a refined control on every single vehicle's trajectory. These methods showed positive results in a model study and simulation validation. However, there are still some problems. The first one is most of the proposed methods rely on a high market penetration rate of control device deployment. The proposed model and validation mostly required fully automated control of participated vehicles. Secondly, although some of these methods allow coordinated control between mainline and onramp vehicles, the coordination can still be improved as more precise and efficient. Meanwhile, these researches hardly consider the impact of complicated traffic circumstances such as mixed vehicle types (CV, AV, and Manual Vehicle (MV)) with different compliance and controllability scale. In this meaning, the control strategy will vary as considering the disturbance among the different types of vehicles with different control-scale. These existing problems prompt the new wave of researches on Connected-Automated-Vehicle (CAV) based DMA methods.

There are several problems to be addressed as considering the existing research:

1) Consider a mixed traffic with fully connected automated vehicle (i.e. CAV), connected but manually controlled vehicle (i.e. CV), and potentially participated disconnected manually controlled vehicle (i.e. MV), what's the DMA model to improve the safety and mobility of all the vehicles while they participated in the control system at a different level?

2) If a DMA method will be designed and applied in mixed traffic, is there any difference between the control algorithms for the vehicles with different control scale?

3) What's a more efficient procedure to choose the mainline gap and on-ramp merging vehicle in different categories (MV, CV, CAV) to group up for a coordinated control?

1.2 Research Objectives and Scope of Work

Based on the above status of current DMA research, the objectives of this research are as follows:

1. Find an efficient and effective way to associate on-ramp merging vehicle and mainline gap, and pair them for a coordinated merging process.

2. Define the features of AV, CV, and MV in respect of automated scale and response to the system signal and adjust the vehicle-gap pairing method to be pervasive to the mixed traffic.

3. Consider the control scale of AV, CV, and MV, and develop a coordinated merge control algorithm for both on-ramp vehicle and mainline gap.

4. Evaluate the performance of the proposed DMA algorithm using VISSIM-based simulation. Compare the performance of the proposed DMA algorithm with legacy CV/AV-based DMA algorithms.

5. Analyze the effectiveness of the proposed DMA algorithm concerning different composition of the mixed type of vehicles.

6. Analyze the sensitivity of model parameters and a penetration rate of CV/AV vehicles.

7. Explore the possibility of further adjustment of the proposed algorithms based on the local ground truth historical data in the field test and field application.

1.3 Research Contributions

My research contributions are as follows:

1. Proposed a microscopic dynamic merging assistance method for CV, AV, and MV mixed traffic in highway merging and weaving sections.

2. Develop an algorithm to generate an instantaneous virtual trajectory (IVT) for the prediction of the vehicle's potential future trajectory based on its preceding traffic profile.

3. Develop a vehicle-gap coordination algorithm based on the vehicles' IVTs considering different vehicle types (i.e., AV, CV, MV) which may involve.

4. Develop a coordinated control model for the paired on-ramp merging vehicle and the mainline gap that has the superior and pervasive performance for mixed traffic environment than most of the other legacy DMA algorithms.

5. Analyze the sensitivity of CV/AV penetration rate.

6. Analyze the performance in the different combination of vehicle types.

1.4 Organization of the Dissertation

Chapters of my dissertation follow the procedure of my dissertation research.

In chapter 2, literature reviews of merge assistance methods are given. The review includes both macroscopic merge assistance methods and microscopic merge assistance methods. Also, the microscopic assistance methods are summarized by their automated scale and control features. Detail of some primary microscopic methods is reviewed and summarized for comparison.

The proposed methodology includes three parts: IVT prediction, vehicle-gap coordination, and vehicle-gap control. These three parts are described in detail in Chapter 3. For IVT prediction, this research would propose a traffic profile collecting and updating system in the environment with V2I communication and propose an algorithm to predict the vehicles' potential future trajectories according to their current instantaneous preceding traffic data and their vehicle types. For vehicle-gap coordination, this research would first propose an algorithm to evaluate if an on-ramp vehicle and a mainline gap can meet and merge appropriately according to their IVTs. Then, a model will be proposed to pair the vehicles and gaps in the merging/weaving area. For vehicle-gap control, different compositions of vehicle types in a three-vehicle-pair will be discussed respectively, and then different control algorithms for them will be proposed.

Chapter 4 and 5 focus on model calibration, validation, and evaluation. A VISSIM simulation network is built based on the geometry of a real merging/weaving area on the highway. The simulation network and some system parameters are calibrated by the collected ground truth data. The proposed model is tested with assumptions of different AV/CV/MV penetration rate. System parameters also vary for sensitivity analysis.

Meanwhile, two reference algorithms are implemented in the same simulation network for comparisons. The results are summarized and analyzed on their performance in mobility (Travel Time, Delay, Speed Distribution, etc.) and safety (Gap Distribution, Time-to-Collision (TTC), etc.)

In Chapter 6, additional analysis is given to conduct a sensitivity analysis concerning different system parameters (i.e., perception-reaction time) and also AV/CV/MV penetration rate.

Finally, the conclusion is drawn, and recommendation for application and deployment of the proposed DMA models will be discussed in Chapter 7.

2   Literature Review

2.1 Overview of Macroscopic Merging Assistance Methods

Existing macroscopic merge control strategies attempt to manipulate the mainline through vehicles or the merging vehicles in the merge section (Scarinci & Heydecker, 2014). Based on the classification by the FHWA, these control principles could be grouped into three categories: "Go Slow to Go Fast," "Keep Sufficient Gaps," and "Zippering" (Margiotta, Spiller, & Halkias, 2007). Those basic concepts have been developed into several types of macroscopic merge control systems.

- Early Merge (EM): Early merge systems are primarily designed to increase safety during the high-speed merge. Vehicles are encouraged to merge early in the auxiliary lane to avoid hazardous conditions towards the end of the auxiliary lane. The most notable system is The Michigan DOT developed a dynamic merge system called the Dynamic Early Lane Merge Traffic Control System (DELMTCS) implemented by Michigan Department of Transportation (Datta, Schattler, Kar, & Guha, 2004).

- Late Merge (LM): Kang et al. (Kang, Chang, & Paracha, 2006) evaluated dynamically late merging in Maryland. They found higher throughput, more equal-lane-volume distribution, and lower maximum queue length when compared to the conventional merging condition. Pesti et al. (Pesti et al., 2008), McCoy and Pesti (Pesti & McCoy, 2001), and later Grillo et al. (Grillo, Datta, & Hartner, 2008) further explored the dynamic late-merging system in which LM is triggered only during the low-speed condition.

- Dynamic Merge (DM): DM strategy is an adaptive strategy that switches between different merge control modes based on the prevailing traffic conditions. Meyer (Meyer, 2004b) used real-time traffic monitoring to test the use of changeable message signs to switch between early merging, late merging, and incident mode during construction along a Kansas highway.

- Dynamic Lane Control (DLC): DLC strategies opens and closes both mainline and entrance ramp lanes to allow for smoother integration of ramp traffic onto the mainline. Notable system design can be found in (Hellernan, June 8, 2010)

- Gap Metering (GM): GM is a merging control strategy proposed by Jin et al. (Peter J. Jin et al., 2016). Gap metering is considered as a mainline version of the ramp metering, but it does not stop the mainline traffic flow unlike earlier implementation in the 1970s and 1990s (Piotrowicz & Robinson, 1995). The concept of GM is to utilize the gaps on the mainline by encouraging the mainline vehicles to yield an efficient gap to allow one merging vehicle to merge in. Simulation studies for the I-35 Riverside corridor in Austin indicate that the gap metering system can significantly reduce the merging delay and network delay even at low penetration rate. The limitation of the GM method is in the macroscopic control strategies. It mainly relies on static or dynamic message signs to convey the control messages. Different mainline drivers can have different interpretations of yielding behavior; different ramp drivers can have their preference for gap selection. All these factors can lead to potentially wasted gaps created by mainline vehicles reducing the through lane capacity.

2.2 Overview of Microscopic Merging Assistance Methods

Some pioneer researches can date back to the 1970s. Since ramp control (RC) (e.g., ramp metering) was a hot topic in highway traffic management in that period, the methods of extending RC strategies to merging assistance system were widely discussed. Buhr (Buhr, Radke, Kirk, & Drew, 1969), Bushnell et al. (Bushnell, 1970), True (True & Rosen, 1973) and Tignor et al. (Tignor, 1975) separately contribute to researches on freeway moving-merge system which made the rate of entry of ramp vehicles to be controlled in some manners in order to fit merging vehicles into a mainline gap. Bauer and Risher (Bauer & Risher, 1977) also did a simulation analysis of the model. Meanwhile, Klee turned his vision to synchronizing the onramp vehicles and mainline gaps. Klee's research (Klee, 1973) considered the interaction between vehicles involved in a merging process and adopted a synchronizing algorithm to improve merging.

After the 1990s, along with the development of the concept of automated highway system (AHS), researchers have turned their focuses to more microscopic and accurate control methods due to the availability of automated control on each vehicle. Hedrick, Tomizuka, and Varaiya (Hedrick, Tomizuka, & Varaiya, 1994) researched on the control issue in AHS and proved the feasibility of implementation of merging control in these systems. Hall and Tsao (Hall & Tsao, 1997) discussed the merging efficiency in AHS and evaluated the merging capacity that this system could increase. Kachroo and Li (Kachroo & Li, 1997) discussed the control laws for onramp merging vehicle in AHS and made an effort in developing the desired behaviors of merging vehicles based on the merging quality and safety which is evaluated by main traffic's speed and position. Antoniotti, Desphande, and Girault (Antoniotti, Desphande, & Girault, 1997) focused on the merging control in

AHS and proposed several detailed stages in the control process. Miller, Misener Godbole and Deshpande (Miller, Misener, Godbole, & Deshpande, 1999) completed some case studies of implemented AHS on Houston Katy Freeway. Ran, Leight, and Chang (Ran, Leight, & Chang, 1999) completed a simulation model for merging control on a dedicated-lane AHS. Lu, Tan, Shladover, and Hedrick(Lu, Tan, Shladover, & Hedrick, 2004) studied a merging maneuver implementation in AHS by focusing on obtaining a smooth merging speed of ramp vehicles based on the speed of main traffic while mainline vehicles were controlled to keep the gap.

Along with the development of autonomous vehicle technologies (e.g., ACC/CACC, etc.) and connected vehicle technologies, these new technologies have emerged in research vision especially in recent years. Autonomous vehicle technologies provide refined control methods on individual vehicles including ACC/CACC based methods (e.g. (Davis, 2007; Scarinci, Heydecker, & Hegyi, 2015; Zhou, Qu, & Jin, 2017)) and other automatic controller-based methods (e.g. (Letter & Elefteriadou, 2017; Milanés, Godoy, Villagrá, & Pérez, 2011; Rios-Torres & Malikopoulos, 2017b; Xie, Zhang, Gartner, & Arsava, 2017)). Connected vehicle technologies enhance these automated control methods by taking advantage of the Vehicle-to-X (V2X) communication. The CV technologies lead to a better awareness of traffic environment and a better delivery of control signals directed towards the drivers or vehicle controllers(Hayat, Park, & Smith, 2014; Letter & Elefteriadou, 2017; Marinescu, Čurn, Bouroche, & Cahill, 2012; Marinescu, Čurn, Slot, Bouroche, & Cahill, 2010; Milanés et al., 2011; Park, Bhamidipati, & Smith, 2011; Park, Su, Hayat, & Smith, 2014; Rios-Torres & Malikopoulos, 2017a, 2017b; Xie et al., 2017; Zhou et al., 2017).

Table 1 shows the features of some representative C/AV-based methods. These methods can take control or provide guidance at different stages during the merging process. The range where the models make decision and control vehicles varies from short-range(Davis, 2007) to medium-(Peter J Jin, Fang, Jiang, DeGaspari, & Walton, 2017; Xie et al., 2017) and long-range(Hayat et al., 2014; Jiang et al., 2017; Letter & Elefteriadou, 2017; Marinescu et al., 2012; Marinescu et al., 2010; Milanés et al., 2011; Park et al., 2011; Park et al., 2014; Rios-Torres & Malikopoulos, 2017a, 2017b; Zhou et al., 2017).

2.3 Representative Microscopic C/AV-based DMA Methods

This section summarizes some existing representative Dynamic Merging Assistance (DMA) methods which are based on connected and/or automated vehicle technologies. These models are presented as three categories: AV-based models, CV-based models, CAV-based models. The focuses of summarizing these models are: 1) the detail algorithms and processing steps; 2) the control targets; 3) the control signal types; 4) the performance evaluation.

Table 1 Comparison of some existing DMA models

Year	Author	Control Target	Control Method	Determination Range	Coordinated Control	Penetration Rate Analysis
2007	Davis	Ramp and Mainline	CACC	Short – Nearby Vehicles Only	Yes	Yes
2010, 2012	Marinescu, et al.	Ramp and Mainline	CAV – AV Control with Communication	Long – Whole Area	Yes	No
2011	Milanes	Ramp and Mainline	CAV - Fuzzy Controller with Communication	Long – Whole Area	No	No
2011, 2014	Park, Hayat, et al.	Mainline	CV – Lane Change Advisory	Long – Whole Area	No	Yes
2014	Park, et al.	Ramp and Mainline	CV – Lane Change Advisory & Speed Guidance	Long – Whole Area	Yes	Yes
2016	Rios-Torres, et al.	Ramp and Mainline	CAV – Fuel-Consumption Optimized Acceleration	Long – Whole Area	Yes	No
2016	Zhou, et al.	Ramp and Mainline	Cooperative AV – Cooperative IDM	Long – Whole Area	Yes	Yes
2016	Xie, et al.	Ramp and Mainline	CAV – Non-linear Optimized Velocity Profile	Medium – Fixed Range	Yes	No
2017	Letter, et al.	Ramp and Mainline	CAV – AV Control with Designed Trajectories	Long – Whole Area	Yes	No

2.3.1 Davis Cooperative Merging Model

In this AV-based research proposed by Davis (Davis Model) (Davis, 2007), a cooperative merging control model with an ACC control is adopted on both mainline traffic and onramp vehicles. Although the system could take control throughout the acceleration lane and take advantages of the data of vehicles on several lanes, it only controlled the vehicles as a cooperative group in a very short range. Thus, I categorize this model as a representative short-range AV-based model. The model's algorithm takes the following steps:

Step 1: Vehicle Dynamics Calculation

The author proposed an ACC model to control a ramp vehicle v_n.

$$\bar{u}_n(t + \Delta t) = \tau \frac{du_n(t)}{dt} + u_n(t) = U(\Delta x_n(t), \Delta u_n(t)) \tag{1}$$

Where $\Delta x_n(t), \Delta u_n(t)$ is the space headway and speed difference between the vehicle v_n and its preceding vehicle v_{n-1}.

$$U(\Delta x_n(t), \Delta u_n(t)) = \frac{1}{h_d}(\Delta x_n(t) - D + \tau \Delta u_n(t)) \tag{2}$$

Where h_d is time headway. A modified version to avoid unnecessary deceleration caused by a cut-in is given as:

$$u_n(t + \tau) = \tau \frac{du_n(t)}{dt} + u_n(t) = \left(u_m(t) - U(\Delta x_n(t), \Delta u_n(t))\right) e^{(-(t-t_m)/t_{relax})} +$$

$$U(\Delta x_n(t), \Delta u_n(t)) \tag{3}$$

Where $u_m(t)$ is the velocity of the cut-in vehicle at the time t_m, $t_{relax} = 6s$ is a relaxation time. A crash-avoidance mechanism is also adopted in the proposed model as follow.

$$\Delta x_n(t) + \frac{u_{n-1}^2(t) - u_n^2(t)}{2a_g} - t_d u_n(t) < D \qquad (4)$$

Where, $D = 7\ m,\ a_g = 3m/s^2,\ t_d = 0.75s$

Step 2: Cooperative Merging

Cooperative merging model controls both mainline and merging vehicles. The formulations are as follows

Mainline Lagging Vehicle in a Gap (PF):

$$U^R(t) = [x_R(t) - x_{p_f}(t) - D - \tau\left(u_R(t) - u_{p_f}(t)\right)]/h_{d1} \qquad (5)$$

When $U^R(t) < U(\Delta x_{p_f}(t), \Delta u_{p_f}(t))$, the desired speed of the mainline lagging vehicle is replaced by

$$\overline{U}_{pf}(t) = \alpha U^R(t) + (1 - \alpha)U(\Delta x_{p_f}(t), \Delta u_{p_f}(t)) \qquad (6)$$

Where, $x_R(t)$ represents the position of nearest merging vehicle R, and $u_R(t)$ is its speed. h_{d1} is headway time, and

$$\alpha = 1 - \frac{x_{pf}(t) + d_{merge}}{L_{CV}} \qquad (7)$$

Where, L_{CV} is the length of the whole covered area, and d_{merge} is the length of the the acceleration lane

Onramp Merging Vehicle:

$$U^{p_l}(t) = [x_{p_l}(t) - x_R(t) - D - \tau\left(u_{p_l}(t) - u_R(t)\right)]/h_{d1} \qquad (8)$$

When $U^{p_l}(t) < U(\Delta x_R(t), \Delta u_R(t))$, the desired speed of the mainline lagging vehicle is replaced by

$$\bar{U}(t) = \alpha U^{p_l}(t) + (1 - \alpha)U(\Delta x_R(t), \Delta u_R(t)) \tag{9}$$

Where $x_{p_l}(t)$ represents the position of the nearest mainline leading vehicle PL, and $u_{p_l}(t)$ is its speed.

Step 3: Rules for Merging

A set of rules has been proposed in this research to describe how the merging vehicles decide to merge into a gap. The on-ramp vehicle R is permitted to change lanes only if the following condition holds:

$$\begin{cases} d_f = x_{p_l}(t) - x_R(t) + \Delta t * \left(u_{p_l}(t) - u_R(t)\right) > S_f * H_{OV}(u_R(t)) \\ d_b = x_R(t) - x_{p_f}(t) + \Delta t * \left(u_R(t) - u_{p_f}(t)\right) > S_f * H_{OV}(u_{p_f}(t)) \end{cases} \tag{10}$$

Where, $S_f = 0.7$ is a safety factor, and H_{OV} is the equilibrium headway at a given velocity in the original optimal velocity model of Bando et al.

When all vehicles are AV, the merging rule can be replaced by:

$$\begin{cases} d_f = x_{p_l}(t) - x_R(t) + \Delta t * \left(u_{p_l}(t) - u_R(t)\right) > u_R(t) * h_{d1} + D \\ d_b = x_R(t) - x_{p_f}(t) + \Delta t * \left(u_R(t) - u_{p_f}(t)\right) > u_{p_f}(t) * h_{d1} + D \end{cases} \tag{11}$$

2.3.2 Marinescu et al.'s Model

This CAV-based research (Marinescu Model) (Marinescu et al., 2012; Marinescu et al., 2010) proposed a vehicle-to-slot (VTS) algorithm to assist on-ramp vehicles in merging into mainlines. The system that Marinescu developed is based on the sensor data such as

GPS point, and it controls the mainline vehicles in a pre-defined behavior. Thus, the trajectories of these vehicles can be accurately predicted, which provides a possibility of finding a mainline slot for an onramp vehicle who will replicate the driving behavior of slot and approach it. The onramp vehicle's entry to the highway is also controlled by a ramp control signal such as ramp metering. The VTS algorithms can be concluded as the following flow chart:
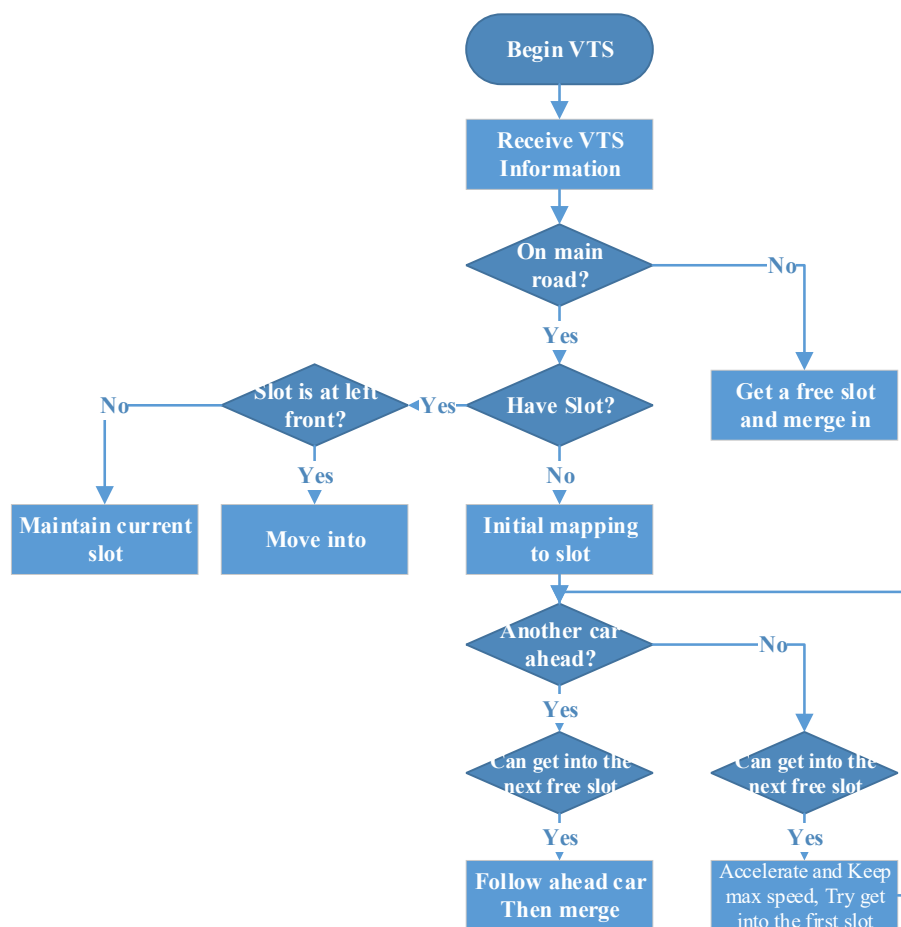
Figure 2 VTS Algorithm in Marinescu Model

2.3.3 Milanes et al.'s Research

Milanes et al. (Milanés et al., 2011) researched the application of V2I communication in merging assistance system. In his research, the potential merging conflicts can be detected and sent to vehicles via V2I communication, and a fuzzy controller is employed in vehicle longitude control. Milanes et al. also conducted experiments to test the prototype vehicles and local control stations

2.3.4 Park et al.'s Model

This CV-based research (Park Model) (Park et al., 2011) proposed equations of motion to model vehicle dynamic. Based on it, the space headway in target time as a gap for merging can be estimated. If the estimated space headway is shorter than the minimum safety distance, the mainline lagging vehicle will receive a lane-change advisory signal. The mainline vehicle drivers who receive lane-change advisory messages may be compliant to open-up more space for merging vehicle. The lane-change advisory decision is made based on the status of vehicles and gaps collected via CV network. This model doesn't actually control any vehicles. However, it takes advantages of the data of vehicles all through the merging area in the long range. Thus, I categorize this model as a representative CV-based model. The algorithm of this model has three steps:

Step 1: Vehicle Dynamic & Target Space Headway Calculation

The calculation of targeted spacing as the following

$$h_{target} = h_{current} + x_{P_l} - x_{P_f} \tag{12}$$

$$(21)$$

Where $h_{current}$ and h_{target} are the prevailing and targeted spacing for R, x_{R-P_l}, x_{R-P_f} are

respectively the distance from r to P_l and P_f respectively. Then, the author proposed three

dynamic cases for gap approaching by R. The signals for the three cases are as follows

Case 1 Acceleration:

$$a = \kappa e^{-\eta v_i} \tag{13}$$

$$v_f = \frac{1}{\eta} \ln(e^{\eta v_i} + \kappa \eta t_{lc}) \tag{14}$$

$$x_f = \frac{1}{\kappa \eta^2} [e^{\eta v}(\eta v - 1)]_{v_i}^{v_f} \tag{15}$$

Case 2 Keep a Constant Speed:

$$a = 0 \tag{16}$$

$$v_f = v_i \tag{17}$$

$$x_f = v_i * t_{lc} \tag{18}$$

Case 3: Deceleration for Cars:

$$a = constant = -11.2 \, ft/s^2 \tag{19}$$

$$v_f = \max(v_i + a(t_{lc} - \tau), 0) \tag{20}$$

$$x_f = v_i \tau + \frac{v_f^2 - v_i^2}{2a} \tag{21}$$

where a is forward direction acceleration, κ, η are parameters for acceleration equation, for

cars, $\kappa = 11.5$ and $\eta = 0.01266$ and for trucks $\kappa = 7.1$ and $\eta = 0.02693$, v_i and v_f are

the speed at the initiation and the completion of lane-changing, t_{lc} is the time duration of a lane change, x_f is the location at lane change completion, and τ is the reaction time.

Step 2: Critical Gap Size Calculation

The critical gap size for lane-changing decision is then defined as the following.

$$Min. \; Safe \; Gap \; h_{safe} = l_{P_l} + (CC0 + CC1 \left(\max \left(v_{P_f} - v_{P_l}, 0 \right) \right))(1 - SRF) \qquad (22)$$

where l_{P_l} is the length of the leading vehicle, $CC0 = 1.5 \, m$, $CC1 = 0.9 \, m$ are Wiedemann car-following model's parameters in VISSIM, $SRF = 0.6$ is safety reduction factor for VISSIMS lane-changing model.

Step 3: Control Decision Making

The lane-changing advisory decision is then made by:

$$h_{target} < h_{safe}$$

2.3.5 Rios-Torres Model

Rios-Torres and Malikopoulos conducted a detailed survey on the CAV coordination control at an intersection and merging at highway on-ramps(Rios-Torres & Malikopoulos, 2017b). Then they proposed an automated and cooperative merge control method(Rios-Torres & Malikopoulos, 2017a) to achieve smooth traffic flow without stop-and-go driving at merging area. The proposed method is based on an optimization framework which minimizes the fuel consumptions. A simulation was conducted to validate the proposed method. The optimization framework was modeled as:

Vehicle Fuel Consumption:

$$\dot{f}_v = \dot{f}_{cruise} + \dot{f}_{accel} \tag{23}$$

$$\dot{f}_{cruise} = q_0 + q_1 * v(t) + q_2 * v^2(t) + q_3 * v^3(t) \tag{24}$$

$$\dot{f}_{accel} = u(t) * (r_0 + r_1 * v(t) + r_2 * v^2(t)) \tag{25}$$

In which, f is estimated fuel consumption, $v(t)$ is speed, and $u(t)$ is acceleration. q, r are parameters which are calculated from experimental data. Thus, the control problem for vehicle in order $N(t)$ can be formulated as:

$$min_{u_i \in \mathbb{R}_i} \left(\frac{\omega_1}{2} \sum_{i=1}^{N(t)} \int_{t_i^0}^{t_i^f} u_i^2(t) dt + \omega_2 \sum_{i=2}^{N(t)} \left| t_i^m \left(u_{(1:i)}(t) \right) - t_{i-1}^m (u_{(1:i-1)}(t)) \right| \right) \tag{26}$$

s.t.:

$$\dot{p}_i = v_i(t), \forall i \in N(t) \tag{27}$$

$$\dot{v}_i = u_i(t), \forall i \in N(t) \tag{28}$$

$$\Gamma_i \cap \Gamma_i = \emptyset, \forall t \in [t_i^0, t_i^f], \forall i, j \in N(t), i \neq j \tag{29}$$

$$\Gamma_i \cong (p_i(t)|p_i(t) \in [L, L+S], \forall i \in N(t), |N(t)| > 1, \forall t \in [t_i^0, t_i^f]) \tag{30}$$

$$t_i^m = t_i^f - \frac{S}{v_i(t_i^f)} \tag{31}$$

Where ω_1, ω_2 are weighting factors to normalize the two terms in equation (29). p_i is position. t_i^f is the time that each vehicle exits the merging area.

2.3.6 Zhou et al.'s Model

Zhou et al. (Zhou et al., 2017) proposed a Vehicle-to-Vehicle (V2V) based cooperative intelligent driver model to maximize merging efficiency. They firstly modeled the human driver behavior by presenting a Full Velocity Difference Model (FVDM) as:

$$a_n(t) = a[V(\Delta x) - v_n(t)] + \lambda\Theta(s_c - \Delta x) \times \Delta v \tag{32}$$

Where a_n denotes the acceleration rate of the n_{th} vehicle at time t; a is the sensitivity constant; $v_n(t)$ is the velocity; $V(\Delta x)$ is an empirical optimal velocity function; λ is asensitivity factor; $s_c = 100\ meters$; $\Theta(x)$ denotes the Heaviside Function; Δx denotes the distance difference from the preceding vehicle; and Δv is the difference of the leader's velocity relative to the follower(Zhou et al., 2017).

Then the behavior of autonomous vehicles was modeled as an optimal velocity and safe headway car-following process which is presented as a Cooperative Intelligent Driver Model (CIDM). The acceleration of intelligent driver model (IDM) in this research is modeled as:

$$a_n(t) = a\left[1 - \left(\frac{v_n}{v_0}\right)^4 - \left(\frac{s^*(v_n,\Delta v_n)}{\Delta x}\right)^2\right] \tag{33}$$

$$s^*(v_n,\Delta v_n) = s_0 + \max[0, v_n T + \frac{v_n \Delta v_n}{2\sqrt{ab}}] \tag{34}$$

In which, s_0 is the minimum distance for vehicles in low-velocity circumstance; a denotes the same parameters in equation (33) that represents the maximum acceleration; T is a safe time gap; b is the desired deceleration rate.

The proposed CIDM model splits the IDM's a_n into:

$$a_n(\Delta x, v_n, \Delta v_n) = a_n^{free} + \sum_m^{n-1} a_{nm}^{int}(\Delta x_{nm}, v_n, \Delta v_{nm}) \qquad (35)$$

$$a_{brake}(\Delta x, v_n, \Delta v_n) = -a\left(\frac{s^*}{\Delta x}\right)^2 \qquad (36)$$

$$a_{free}(\Delta x, v_n, \Delta v_n) = a[1 - \left(\frac{v_n}{v_0}\right)^4] \qquad (37)$$

In which a_{nm}^{int} is a_{brake} with the consideration of vehicle-vehicle interaction, and a_n^{free} has the same definition as a_{free} above.

Based on the derived AV control model, some additional cooperative rules were proposed for more practical cooperative driving behavior:

Exponential Moving Average (EMA):

$$x_{EMA}(t) = \frac{1}{\tau}\int_{-\infty}^t e^{-\frac{t-t'}{\tau}} x(t')dt' \qquad (38)$$

Lane-Changing Impact (LCI):

$$\lambda_{\Delta x} = \max\left[0.4, \left(\frac{\Delta x_0(t)}{R_d}\right)^2\right], \Delta x_0(t) < R_d, \Delta x = \lambda_{\Delta x} * \Delta x \qquad (39)$$

2.3.7 Xie et al.'s Model

Xie et al. (Xie et al., 2017) proposed a collaborative merging assistance method for on-ramp connected and autonomous vehicles. The proposed ramp control strategy is a constrained nonlinear optimization problem which provides individual vehicles with step-by-step control instruction. The optimization problem was modeled as:

$$Min(-\alpha \sum_{i=1}^{2} \sum_{s=1}^{n_i} \sum_{k=1}^{m} v_{i,s,t_k} + \beta \sum_{i=1}^{2} \sum_{s=1}^{n_i} SD_{i,s}) \tag{40}$$

s.t.:

$$0 \leq v_{i,s,t_k} \leq v_{max} \quad \forall i, s, k \tag{41}$$

$$G_{min} \leq |x_{i,s,t_k} - x_{i,s-1,t_k}| \quad \forall i, k; s = 2, \dots, n_i \tag{42}$$

$$G_{min} \leq |x_{1,j,m} - x_{2,p,m}| \quad \forall j = 1, \dots, n_1; p = 1, \dots, n_2 \tag{43}$$

$$|a_{i,s,t_k} - a_{i,s,t_{k+1}}| \leq a_{mx_{diff}} \quad \forall i, s; k = 1, \dots, m-1 \tag{44}$$

$$\frac{x_{i,s,t_{k+1}} - x_{i,s,t_k}}{t_{k+1} - t_k} = v_{i,s,t_k} \tag{45}$$

$$\frac{v_{i,s,t_{k+1}} - v_{i,s,t_k}}{t_{k+1} - t_k} = a_{i,s,t_k} \quad \forall i, s; k = 1, \dots, m-1 \tag{46}$$

$$a_{min} \leq a_{i,s,t_k} \leq a_{max} \quad \forall i, s, k \tag{47}$$

Where i is lane identifier (1-freeway right lane and 2-ramp); j is index for vehicles on the freeway; p is index for vehicles on the ramp; s is index for vehicles irrespective of whether they are on the ramp or the freeway; k is the time step index; m is the total number of time steps; n_i is the total number of vehicles in upstream links of merging zone; t_k is the k_{th} time step; a_{i,s,t_k} is the acceleration of vehicle s in lane i at time step t_k; v_{i,s,t_k} is the velocity; x_{i,s,t_k} is the distance to the merging point; v_{max} is the speed limit; G_{min} is minimum distance gap; a_{min} is minimum acceleration rate; a_{max} is maximum acceleration rate; a_{mx_diff} is maximum accelerate change between two consecutive time steps. $SD_{i,s}$ is the standard deviation of accelerations for vehicle s in lane i; α, β are weighting factors.

A VISSIM based simulation was conducted for validation. The proposed model was implemented with VISSIM COM interface and Car2X application.

2.3.8 Letter & Elefteriadou's Model

Letter et al.(Letter & Elefteriadou, 2017) (Letter Model) proposed a trajectory optimization algorithm to maximize the average vehicle speed on the ramp and the target lane. The algorithm is designed for fully connected and automated vehicles with the consideration of the potential vehicle arrival sequence from the ramps and target lanes. The proposed model is evaluated by a simulation study for a hypothetical merge section consisting of a one-lane mainline with a 107-meter (350-feet) acceleration lane and a one-lane ramp. This model implements a refined automated control on all vehicles and takes advantages of the data of all vehicles all through the merging area. Thus, I categorize this model as a representative connected automated-based model. The algorithm of this model can be summarized as:

Step 1: Vehicle Ordering for Trajectory Calculation

For all mainline and merging vehicles which are not processed and assigned trajectories, calculate their order of merging based on their potential arrival time to the merge point. The vehicles will be controlled to accelerate or decelerate to accommodate a selected merge speed.

Step 2: Solve an Optimization Problem for Trajectories Generation

An optimization problem is proposed to generate a trajectory which can maximize all vehicles' average travel speed.

Objective Function: Minimize average travel speed: $maxZ = \frac{\Sigma V_i}{n+1}$ (48)

Decision Variable: Acceleration: A_i

Constrains:

Safe Time Gap Constrain: $\frac{X_i - Y_i}{V_i} \geq h_s$ (49)

Velocity Constrain: $V_i \leq mergeSpeed, \; V_i \geq 0$ (50)

Acceleration Constrain: $A_i \leq a * V_i + b, \; A_i \leq maxDecel$ (51)

Jerk Constrain: $|A_i - A_{i-1}| \leq maxJerk$ (52)

3 Methodology

This dissertation designs a CAV-V2I-based merge assistance system. The system will generate Instantaneous Virtual Trajectories (IVT) for both mainline and onramp C/AVs based on the instantaneous traffic condition within the control area. IVT is used to predict the vehicles' merging potential based on which the mainline gap and on-ramp vehicle (vehicle-gap pair) can be paired. Then the vehicle-gap pair are synchronized by a coordination control to achieve an efficient and safe merge. The proposed system can work in a mixed traffic environment through deriving different control strategies for all possible combination scenarios among MV, CV, and AV which takes different roles during merge activity (i.e., mainline pseudo-leading (PL) vehicle p_l, mainline pseudo-following (PF) vehicle p_f and onramp merging vehicle R (R)). Figure 3 shows the control framework.
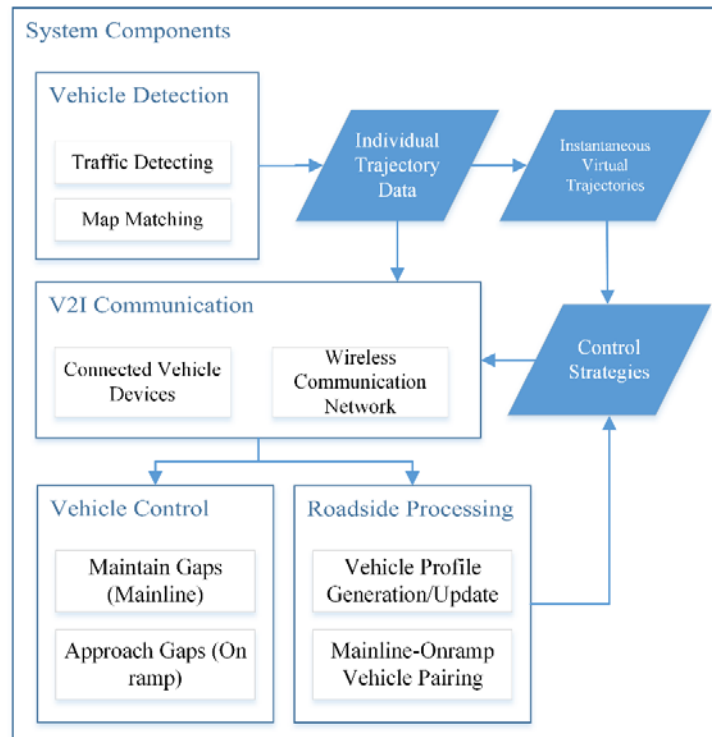
Figure 3 System framework

3.1 System Requirement and Assumptions

The following requirements and assumptions are stated to facilitate the derivation of the DMA control algorithms for mixed traffic.

1) The proposed method is a centralized control system where all information will be gathered in a roadside control center. Thus, V2I communication is necessary to allow vehicles to send information to and receive a control signal (i.e., speed guidance and lane-change signal) from the road-side unit (RSU).

2) Vehicle-to-Vehicle (V2V) communication is not considered in this research because V2V based methods usually work for the applications for a small group of vehicles due to its relatively short communication range and relatively lower quality. In addition, a V2V based method usually requires a higher penetration rate and autonomy level to achieve the same effective area with V2I based method.

3) The status of vehicles (i.e., location, speed, etc.) is detected by the onboard sensors on Connected Vehicles as well as the roadside sensors such as high-angle cameras, roadside LiDAR, etc. This research does not consider the processing of detection data. Thus, the detected vehicle status is assumed as explicit.

4) MV Participants: MVs are not connected via V2I communication and cannot be directly affected by the V2I-Mixed DMA system. They are considered as uncontrollable in this research although they may be compliant to lane-change advisory or gap/ramp metering information shown on roadside variable message sign. However, MVs' location and velocity are still assumed to be detected by

precise detectors such as Remote Traffic Microwave Sensor (RTMS), Video Sensors, or even LiDAR sensors if budget allowed.

5) CV Participants: CVs are manually controlled while it can exchange information with infrastructure and receive speed/lane-change guidance signals from RSU. Considering the non-compliant CV performs similar with MV regarding controllability, I assume that CV mentioned in the research is compliant-CV whose driver will follow the control signals despite a longer perception-reaction time.

6) AVs in this research is CAV connected with V2I communication. Their speed is controlled by the speed guidance sent from V2I-Mixed DMA system which is updated every step.

7) The dynamic merging assistance method in this research is a microscopic method which generates gaps and coordinated speed guidance for each individual vehicle instead of macroscopic traffic control such as ramp metering or gap metering.

8) Although the communication quality is a critical issue in the real-world practice (2013a; 2013b), this theoretical and model-studied research assumes the wireless communication quality as perfect as that the packet loss and communication delay are ignored. Related sensitivity analysis will be part of future work.

3.2 Notation List

i, m, r, t: the index of a link segment, mainline vehicle, onramp vehicle, and time interval respectively.

$(x_k, y_k), (px_k, py_k)$: The global and projected (onto the lane's centerline) coordinates of the vehicle V_k respectively.

$l_i, P_i = (sx_i, sy_i)$: The length of link segment i and the 2-D global coordinates of its starting point respectively.

P_0: The end of the acceleration lane, the origin of linear reference coordinates

ψ: The linear referencing coordinate. This is also the distance toward the end of the acceleration lane P_0.

η_i: The offset from the starting point of link i along the centerline of a lane.

τ_m, ψ_m: the time and linear-reference coordinate of vehicle m on the instantaneous virtual trajectory.

$G_k = (t_k, -\psi_k)$: the instantaneous time and linear-reference coordinate of vehicle V_k.

$\tilde{G}_i^k = (\tau_i^k, -\psi_i(t_0))$: the i_{th} guide-spot's time and linear-reference coordinate on the instantaneous virtual trajectory of the vehicle V_k at time $t_0, 0 \leq i < k$.

$a_k(t), u_k(t)$: the acceleration and velocity of the vehicle V_k at time t

$\bar{a}_k(t + \Delta t), \bar{u}_k(t + \Delta t)$: the desired acceleration and velocity for the vehicle V_k in the next time interval $(t + \Delta t)$.

TL_1, TL_2, TL_3: The required length threshold for three pairing scenarios.

R, P_l (PL), P_f (PF), and R_l (RL): the indexes of the onramp vehicle, the putative leading and following vehicle for a candidate gap, and the direct preceding vehicle of the onramp vehicle, respectively.

L_{CV}: The total coverage length of control area including merging area and upstream ramp/mainline links covered for vehicle-gap pairing preparation.

L_d: The desired gap size.

3.3 Linear-Referencing Coordinate System and Map Matching
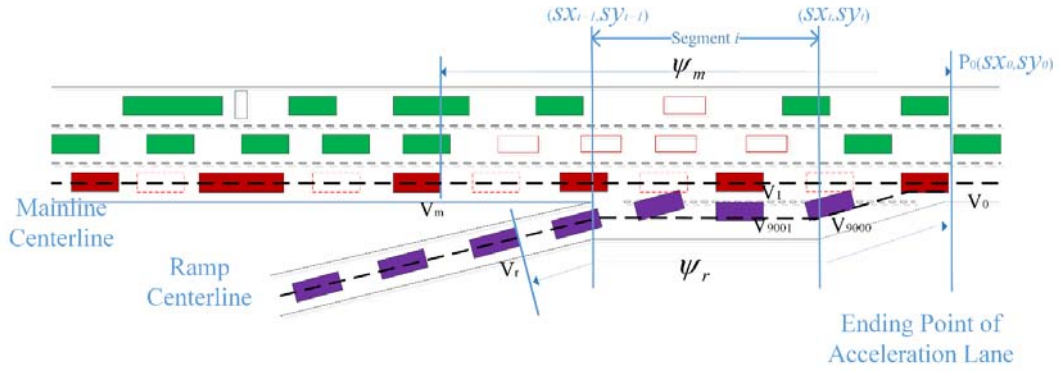
Figure 4 Illustration of the linear-referencing coordinate system.

As illustrated in Figure 4, a linear referencing system is used in this study for vehicle positioning. The linear-referencing coordinate ψ is defined as the accumulative distance along the centerline of each lane from the endpoint P_0 of the auxiliary lane. The projection from any upstream location $P^*(x^*, y^*)$ to its linear referencing system coordinate ψ takes the following steps.

Step 1. Calculate the link length based on the projected coordinates of the starting and ending point (sx_i, sy_i) and (sx_{i+1}, sy_{i+1}) on the centerline of a link.

$$l_i = \sqrt{(sx_i - sx_{i+1})^2 + (sy_i - sy_{i+1})^2} \tag{53}$$

Step 2. Calculate the link offset η_i of each upstream location $P^*(x^*, y^*)$ on link i as follows.

Define the perpendicular vector as the following

$$(a, b) = (sy_{i+1} - sy_i, sx_i - sx_{i+1})$$

In order to project the vehicle's GPS point $P^*(x^*, y^*)$ onto the link segment i, the equation

of the perpendicular line of link segment i containing point $P^*(x^*, y^*)$ can be described as:

$$bx - ay + a * y^* - b * x^* = 0$$

Therefore, its projected point (px^*, py^*) on the link segment i can be calculated as the
following.

$$\begin{cases} px^* = y_p * \dfrac{a}{b} - \dfrac{a * y^* - b * x^*}{b} \\ py^* = \dfrac{a^2 * y^* - ab * x^* - b(sx_{i+1}sy_i - sx_i sy_{i+1})}{b^2 + a^2} \end{cases}$$

To check if the projected point (px^*, py^*) is within link segment i, the following

conditions are evaluated.

$$\begin{cases} (sx_i - px^*) * (px^* - sx_{i+1}) \geq 0 \\ (sy_i - py^*) * (py^* - sy_{i+1}) \geq 0 \end{cases} \tag{54}$$

Assuming the projected coordinate is on link J, then the link offset of P on link J equals

the following.

$$\eta_J^* = \sqrt{\left(px^* - sx_J\right)^2 + \left(py^* - sy_J\right)^2}$$

Finally, the linear referencing coordinate ψ^* of $P(x, y)$ can be calculated by the following.

$$\psi = \sum_{i=0}^{J-1} l_i + \eta_J^* \tag{55}$$

3.4 Instantaneous Lane Speed Profiles (ISP) and Instantaneous Virtual Trajectories (IVT)

The mainline and ramp instantaneous speed profile (ISP) at time t are defined as two sets

of speed-location pairs,

$$\begin{cases} ISP_M(t) = \langle u_m; \psi_m; t \rangle \\ ISP_R(t) = \langle u_r; \psi_r; t \rangle \end{cases} \tag{56}$$

where u, ψ are the instantaneous speed and location respectively, and m, r are the indexes of mainline and onramp vehicles at time t. For the convenience of discussion, I assume m and r do not overlap, e.g., all mainline vehicles are indexed as 1,2,3, …, and etc.; while all ramp vehicles are indexed as 9001, 9002,…, and etc.

The instantaneous virtual trajectory (IVT) is introduced to determine the expected merging point for mainline-onramp vehicle pairing and synchronization. The IVTs are generated based on the instantaneous speed profiles of the corresponding mainline through lane or ramps.

The IVT of a vehicle m at time t are defined as piecewise linear function breaking at the guide spots $\{\tau_k, \psi_k; t\}$, where the guide sports are the locations of all preceding vehicles at time t, and $k = 1, \ldots, m_0 - 1$ are the indexes of all preceding vehicles starting from P_0. τ_k is the expected time lapse from the current vehicle position to the predicted trajectory point k on IVT. τ_k is based on the time intervals between two consecutive trajectory points k and $(k + 1)$ if traveling at the speed at the upstream point $(k + 1)$.

$$\tau_m = t + \tau_k = t + \sum_{k=m}^{m_0-1} \frac{|\psi_{k+1}-\psi_k|}{u_{k+1}} \qquad , m \in [0, m_0 - 1] \qquad (57)$$

In which τ_m is the time coordinates; ψ_m is the downstream vehicle veh_m's linear reference coordinate.

Figure 5(a) illustrates a sample IVT for a mainline vehicle. For illustration purposes, I convert the value of spatial coordinates from ψ_i to $-\psi_i$.
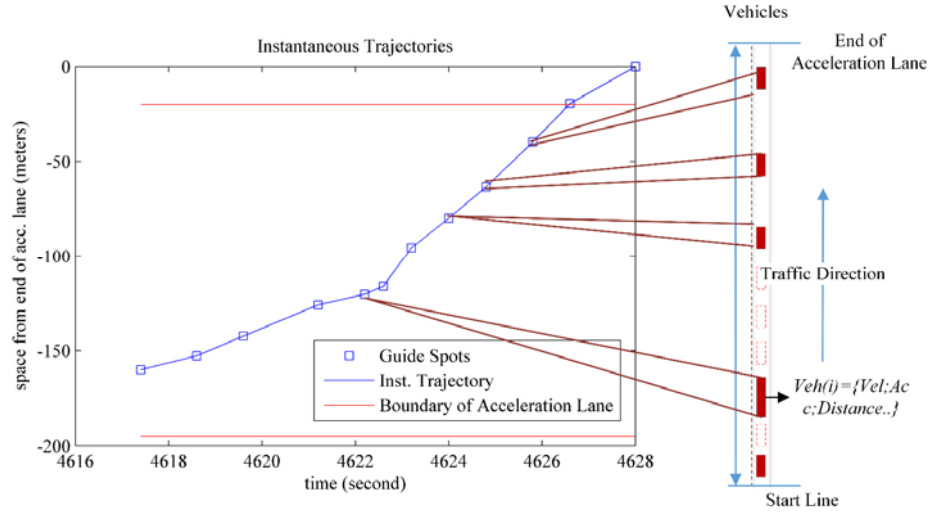
Figure 5 Sample of A Mainline Instantaneous Virtual Trajectory

3.5 Intersection Detection between Mainline and Ramp IVTs

IVTs of mainline vehicles and onramp vehicles can be used to predict whether or not an intersection point within the merging area exists. The intersection detection between two IVTs is conducted in three steps.

Step 1 Quick-Check Potentially Intersections: Given any two segments $MIVT_m \in (MG_m, MG_{m+1})$ in the mainline IVT and $RIVT_n \in (RG_n, RG_{n+1})$ in the ramp IVT, they can be quickly pre-screened to see whether there can be an intersecting point exactly on themselves (instead of on their extension line). If any of the following criteria are satisfied, then no intersection will exist.

$$\begin{cases} \tau_m \le \tau_{r+1} \\ \tau_{m+1} \ge \tau_r \\ \psi_m \le \psi_{r+1} \\ \psi_{m+1} \ge \psi_r \end{cases} \tag{58}$$

Step 2 Identify Parallel or Overlapping IVT Segments: After passing the screening test in Step 1, the two segments also need to be judged for a parallel relationship. The criterion is written as follows:

$$(\psi_{m+1} - \psi_m) * (\tau_{r+1} - \tau_r) = (\psi_{r+1} - \psi_r) * (\tau_{m+1} - \tau_m) \tag{59}$$

If the equation holds, I can judge that the two segments are parallel or overlapped, then I check whether they are overlapped by the following condition.

$$(\tau_{m+1} * \psi_m - \tau_m * \psi_{m+1}) * (\tau_{r+1} - \tau_r) = (\tau_{r+1} * \psi_r - \tau_r * \psi_{r+1}) * (\tau_{m+1} - \tau_m) \tag{60}$$

If Equation (60) holds and overlapping segments are identified, then the entire overlapping area is safe for merging; otherwise, two IVTs are paralleled without any intersecting points exist.

Step 3 Determine Intersection Points: Find the overlapping points by solving the following equation-set to find the intersection coordinates $\tau_m \ and \ \psi_m$

$$\begin{cases} (\tau - \tau_m) * (\psi_{m+1} - \psi_m) = (\psi - \psi_m) * (\tau_{m+1} - \tau_m) \\ (\tau - \tau_r) * (\psi_{r+1} - \psi_r) = (\psi - \psi_r) * (\tau_{r+1} - \tau_r) \end{cases} \tag{61}$$

If the solution (τ_{int}, ψ_{int}) for the Equation set (61) exists, then the intersection point is where the onramp vehicle is safe to merge.

3.6 General Rules for Vehicle-Gap Pairing

Pairing an onramp vehicle with a gap on mainline requires the evaluation of the relationship among the IVTs of two consecutive mainline vehicles (Putative Leader (P_l) and Putative Follower (P_f) of a gap) and the IVT of on an onramp vehicle R. To ensure safety, the trajectories of P_l and P_f needs to be shifted backward and forward for a safe distance d_{safe} before further analysis. There are three pairing scenarios to be considered.

Scenario 1: The IVT_R intersects both two consecutive IVTs within the merging area. The two IVTs are marked then as IVT_{P_l} and VT_{P_f}. In this scenario, there should be sufficient spacing between IVT_{P_l} and IVT_{P_f} to allow the safe merging. Figure 6 shows a schematic

of the scenario, in which the dashed line shows the speed synchronization process with P_l and the round dot is the velocity-synchronized position. Firstly, I can calculate the minimum time that vehicle R will take to synchronize its speed with P_l.

$$\Delta t = \frac{(u_{pm} - u_R)}{A_{rmax}} \tag{62}$$

where u_R, u_{pm} are the velocities of R and P_l (or P_f) when R firstly meets P_l (accelerating merge) or P_f (decelerating merge), respectively, $A_{rmax} = 1.5 \ m/s^2$ if accelerating merge, and $A_{rmax\_dec} = -4 \ m/s^2$. The required accelerate/decelerate distance is calculated by kinematic equations.

$$TL_1 = \begin{cases} u_r * \Delta t + 0.5 * a_{rmax_{dec}} * \Delta t^2 - u_{pf} * \Delta t - d_{safe} - L_r \\ \psi_{pf} - \psi_{pl} + u_r * \Delta t + 0.5 * a_{rmax} * \Delta t^2 - u_{pf} * \Delta t - d_{safe} - L_r \end{cases}$$

$$TL_1' = \begin{cases} u_{pl} * \Delta t + \psi_{pf} - \psi_{pl} - u_r * \Delta t - 0.5 * a_{rmax_{dec}} * \Delta t^2 - d_{safe} - L_{pl} \\ u_{pl} * \Delta t - u_r * \Delta t - 0.5 * a_{rmax} * \Delta t^2 - d_{safe} - L_{pl} \end{cases}$$

$$\tag{63}$$

and for a successful pairing, the following criterion shall be checked:

$$\begin{cases} TL_1 > 0 \\ TL_1' > 0 \end{cases} \tag{64}$$

In which, u_{pf} is the velocity of P_f when R initially meets the gap; L_{pl-pf} is the distance between $P_l \ and \ P_f$ initially meet; L_r is the length of R.

Scenario 2: If IVT_R intersects with only one IVT. I mark this vehicle as P_l. If the intersection is far away enough from the end of the auxiliary lane, this is also an eligible pair. The checking criteria are

$$TL_2 = L_0 - \psi_{int} > L_r \tag{65}$$

Where, L_0 is the length of the acceleration lane.

Scenario 3: If R cannot find any intersections with any mainline vehicles, and the gap between two closest upstream and downstream mainline vehicle IVTs are large enough. It means that the merging section will be quite clear during merging. I still mark the closest upstream vehicle as P_f, then the condition becomes

$$TL_3 = \hat{\psi}_{pf} - d_{safe} > L_r \tag{66}$$

In which $\hat{\psi}_{pf}$ is the remaining distance of P_f toward the end of acceleration lane when P_l reaches the end of the acceleration lane.
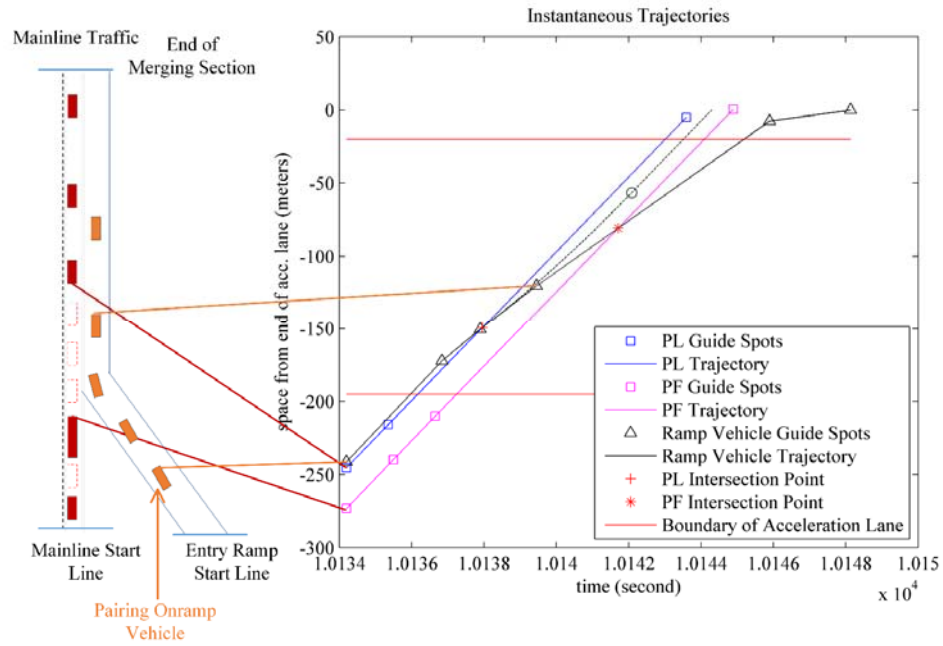
Figure 6 Sample Schema for Instantaneous Virtual Trajectory-based Vehicle-Gap Pairing

3.7 Vehicle-Gap Pairing in Mixed Traffic

3.7.1 Merging scenarios with mixed traffic

Scenario 1 (Type I): Onramp-C/AV PF-C/AV PL-Any

This is the basic and standard scenario. In this scenario, both R and PF are controllable. The control model can take effect on both sides. Regular vehicle-gap pairing criteria and the pair-refresh process are applied. In this scenario, PL is not required to change its behavior during control circles for less disturbance to the mainline traffic. The control strategy and refresh criteria applied to this scenario are defined as Type-I.

Scenario 2 (Type II): Onramp-MV PF-C/AV PL-Any

In this scenario, the on-ramp merging vehicle is MV. It follows a natural human driving style which only considers the physically surrounding vehicles. Meanwhile, PF is still a CV/AV, and it can forwardly yield to the paired merging vehicle. PL is not necessarily involved in control. The mainline control strategy and refresh criteria applied in this scenario are defined as Type-II.
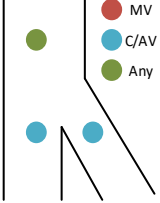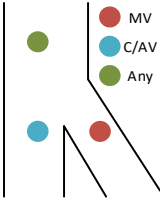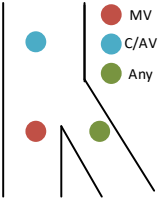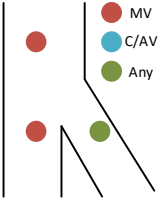
Scenario 3 (Type III): Onramp-Any PF-MV PL-C/AV

In this scenario, the PF-based gap control is not available. However, another type of gap yielding/keeping control can be implemented if PL is controllable. PL can open a gap by forwardly keep a larger distance from its following vehicle. However, PL may participate in another vehicle-gap pair as PF. Thus, this Type-III mainline control strategy shall consider the existing control already implemented on PL.

Scenario 4 (Type IV): Onramp-Any PF-MV PL-MV

In this scenario, the ramp vehicle cannot find a controllable mainline gap. However, it will still be paired with a mainline gap consists of two MV. The regular Type I control-logic is applied to the on-ramp vehicle if it is controllable, and it will keep searching for another controllable gap for better performance.

Table 2 Summary of the different types of vehicle combinations and control modules

		Type I	Type II	Type III	Type IV
Vehicle Combination Scenario					
Paring Criteria	Estimated Merging Status	Basic Pairing - Estimated location when merging	Type I + Merging speed difference	Type II + Larger Gap Length	Type III + Open for another controllable gap
	Mainline Vehicle Availability	Two mainline vehicles who stay in the right lane and be consecutive			
	Target Link Checking	Ramp vehicles targeting merging to mainline instead of local passing-through			
Onramp Control		Basic V2I-DMA Control	N/A	None/V2I-DMA Control	None/V2I-DMA Control
Mainline Control		Basic V2I-DMA Control	Limited V2I-DMA Control	PL-Speed Adjustment	N/A

3.7.2 Rules for Vehicle-Gap Paring in Mixed Traffic

The onramp vehicle R will search for a qualified gap in mainline queue starting from the end side of acceleration lane to implement a "late merge" strategy. R and PL-PF gap are paired based on their status at merging which is predicted by IVTs. The pairing criteria are different for all four scenarios:

- Estimated Merging Status Eligibility: The estimated locations of on-ramp vehicle and the two mainline vehicles at merging time which is predicted by their IVTs will be checked.

  o Type-I: The estimated merging location shall be in the acceleration lane, and the gap between two mainline vehicles shall meet the minimum requirement. This is the basic pairing criteria in the CV-V2I DMA system.

  o Type-II: Besides the criteria in Type-I, the pair shall have a small difference of estimated speed at merging location. Otherwise, it will be unpaired and released due to the disability of R to adjust its speed during the process.

  o Type-III: Besides the criteria in Type-II, a larger gap length is required in Type-III because PF cannot forwardly open gap although a positive gap-opening control is implemented by PL, which may be less efficient than PF.

  o Type-IV: In the scenario, the pair will still be established as Type-III. However, R will keep searching for another controllable gap no matter it is paired or not.

- Mainline Vehicle Availability: PL or PF shall stay in the right-most lane and be consecutive. If they change lane or other vehicles insert into the gap, the vehicle-gap pair will be released.

- Target Link Checking: The on-ramp vehicle whose target link is not mainline (leaving to off-ramp) will not participate in the V2I-Mixed DMA system.

The IVTs of involved vehicles will be detected and estimated dynamically in real-time. If the above criteria do not hold, the Vehicle-Gap pair will be released and start a new search.

3.8 Gap maintaining by mainline vehicles (for PL/PF)

Type I: Basic V2I-DMA Control:

After pairing with an on-ramp vehicle R, PF will forwardly open and maintain a gap privileged for it. The desired velocity for PF comes from two components of the ACC model. The first component, named as "Gap Opening" where PL is counted as the preceding vehicle, is applied for opening and keeping a gap. The second component, named as "Merging Yielding" where R is counted as the preceding vehicle, works for yielding to the merging vehicle. The weight of the two components changes per the distance between PF's current location and the estimated merging location.

- Component 1- Gap Opening: I apply a linear ACC model as:

$$\bar{a}'_{p_f}(t + \Delta t) = K_0 a_{p_l}(t) + K_1 \left(u_{p_l}(t) - u_{p_f}(t) \right) + K_2 (\psi_{p_f} - \psi_{p_l} - l_{p_l} - L_d)$$
$$(67)$$

$$\bar{u}'_{p_f}(t + \Delta t) = u_{p_f}(t) + \bar{a}'_{p_f}(t + \Delta t) * \Delta t \qquad (68)$$

Where $\bar{a}'_k(t + \Delta t)$ ($\bar{u}'_k(t + \Delta t)$) and $a_k(t)$ ($u_k(t)$) are the guidance and prevailing acceleration (velocity) of vehicle k respectively, ψ_k is the distance from vehicle k's current location to the end of acceleration lane respectively , l_{p_l} is the length of P_l, $L_d = 9$ (m) is the desired space distance which is tuned based on trial simulation runs slightly larger than the length of an average passenger vehicle; k_0, k_1 and k_2 are model's design constants.

- Component 2-Merging Yielding: I adopt a proposed ACC model (Davis, 2007) albeit the counted preceding vehicle is R instead of the vehicle physically near P_f.

$$\bar{u}''_{pf}(t + \Delta t) = (\psi_{pf} - \psi_R - L_d)/h_d + \left(u_R(t) - u_{pf}(t)\right) * \Delta t/h_d \qquad (69)$$

$$\bar{a}''_{pf}(t + \Delta t) = (u''_{pf}(t + \Delta t) - u_{pf}(t))/\Delta t \qquad (70)$$

where h_d is headway time.

- Gap Control Signal: The gap control guidance is then generated by applying weights to the above two components as the following.

$$\bar{u}_{pf}(t + \Delta t) = \alpha \bar{u}'_{pf}(t + \Delta t) + (1 - \alpha)\bar{u}''_{pf}(t + \Delta t) \qquad (71)$$

While $\alpha = \dfrac{\psi_{pf} - \psi_{merge}}{L_{CV} - \psi_{merge}}$

Where L_{CV} is the total length of control area including acceleration lane and other upstream links covered by CV network, ψ_{merge} is the distance from the estimated merging location to the end of the acceleration lane.

Type II: Limited V2I-DMA Control:

In this type, the control for mainline vehicles will be less active than Type-I mode because R is uncontrollable and may not catch up with the opened gap in an efficient way. This will lead to a waste of mainline capacity and will require more tolerance from the opened gap regarding gap-length and relative speed. Thus, I adjust the parameter and the trigger time for mainline vehicle control.

- Component 1- Gap Opening:

$$\bar{a}'_{pf}(t + \Delta t) = K_0 a_{p_l}(t) + K_1 \left(u_{p_l}(t) - u_{pf}(t)\right) + K_2 (\psi_{pf} - \psi_{p_l} - l_{p_l} - L_d)$$
$$(72)$$

$$\bar{u}'_{p_f}(t + \Delta t) = u_{p_f}(t) + \bar{a}'_{p_f}(t + \Delta t) * \Delta t \tag{73}$$

Where a longer $L_d = 15$ (m) is the desired space distance which is approximately one vehicle length longer than the one applied in type I.

- Component 2-Merging Yielding:

$$\bar{u}''_{pf}(t + \Delta t) = (\psi_{pf} - \psi_R - L_d)/h_d + \left(u_R(t) - u_{pf}(t)\right) * \Delta t/h_d \tag{74}$$

$$\bar{a}''_{pf}(t + \Delta t) = (u''_{pf}(t + \Delta t) - u_{pf}(t))/\Delta t \tag{75}$$

- Trigger Time: At the early stage of approaching the estimated merging location, the vehicles will drive naturally by itself and only consider its physically nearby vehicles. When P_f arrive at the position which is 50 meters away from the estimated merging location, the mainline control will be triggered and activated.

- Gap Control Signal: The gap control guidance is then generated by applying weights to the above two components as the following.

$$\bar{u}_{pf}(t + \Delta t) = \alpha\bar{u}'_{pf}(t + \Delta t) + (1 - \alpha)\bar{u}''_{pf}(t + \Delta t) \tag{76}$$

While $\alpha = \dfrac{\psi_{p_f} - \psi_{merging}}{50}$, only when $\psi_{p_f} - \psi_{merging} < 50$

Type III: PL-Speed Adjustment:

In this type, p_f and p_r cannot be controlled while p_l is controllable. Thus, I design its behavior as:

- Component 1- Independent Speed: PL may be a part of another Type-I/II controllable gap as the lagging one; thus, it already has an input speed/accelerate signal as:

$$\bar{u}_{pl}'(t + \Delta t) \tag{77}$$

$$\bar{a}'(t) = (\bar{u}_{pl}'(t + \Delta t) - u_{pl}(t))/\Delta t \tag{78}$$

Where $u_{pl}(t)$ is PL's current velocity.

- Component 2 - Following IVT: The current vehicle PL will follow its IVT if it does not participate in another vehicle-gap pair. The speed is:

$$u_{pl}''(t + \Delta t) \tag{79}$$

$$\bar{a}''(t) = (\bar{u}_{pl}''(t + \Delta t) - u_{pl}(t))/\Delta t \tag{80}$$

- Component 3- Elastic Gap Opening: PL adopts a modified ACC model to open a gap for R forwardly. It assumes that PL is following R but trying to keep a "negative gap" to ensure PL is actually ahead with a required gap length.

$$\bar{a}_{pl}'''(t + \Delta t) = K_0 a_R(t) + K_1 \left(u_R(t) - u_{pl}(t) \right) - K_2 \left(\psi_R - \psi_{pl} - l_{pl} - L_d \right) \tag{81}$$

$$\bar{u}_{pl}'''(t) = u_{pl}(t) + \bar{a}_{pl}'''\Delta t \tag{82}$$

- Gap Control Signal: The gap control guidance is then generated by applying weights to the above three components as the following.

$$\bar{u}_{pl}(t + \Delta t) = \alpha * \left(\omega \bar{u}_{pl}'(t + \Delta t) + (1 - \omega)\bar{u}_{pl}''(t + \Delta t) \right) + (1 - \alpha) * \bar{u}'''(t + \Delta t) \tag{83}$$

While $\alpha = \frac{\psi_{pl} - \psi_{merging}}{50}$, only when $\psi_{p_f} - \psi_{merging} < 50$. $\omega = 1$ when PL participates another vehicle-gap pair as PF, otherwise $\omega = 0$.

3.9 Gap approaching by onramp vehicle (for on-ramp C/AV R in all type)

Gap approaching algorithms consist of a crash-void car-following model with P_{rl} and the gap approaching model towards the targeted gap. The actual approaching speed/acceleration are determined by one of them which is smaller.

- Car-Following-Signal: Although R is controlled to approach the paired gap, it is actually driving on another lane with another physically preceding car. Thus, the Gipps Car-following model is used to form a natural car-following(Gipps, 1981).

$$\bar{u}_R^{cf}(t + \Delta t) =$$

$$\min \begin{cases} u_R(t) + 2.5a_R\Delta t \left(1 - \frac{u_R(t)}{U_i}\right) \sqrt{0.025 + \frac{u_R(t)}{U_i}} \\ -b\Delta t + \sqrt{b^2\Delta t^2 + b\{2[\psi_R(t) - l_{R_L} - L_d - \psi_{R_L}(t)] - u_R(t)\Delta t + (u_{R_L}(t)^2)/b'\}} \end{cases}$$

$$a_r^{cf}(t + \Delta t) = \left(\bar{u}_R(t + \Delta t) - u_R(t)\right)/\Delta t \tag{84}$$

where a_r^{cf} is the desired acceleration of onramp vehicle (m/s^2) for the crash-void car-following model, Δt is the system's reaction time varied with the type of vehicle (s); U_i is the desired speed (m/s) on link i which is a preset parameter for each link, b is the actual maximum deceleration of the vehicle, b' is the estimated maximum deceleration the preceding vehicle is willing to employ, l_R is the length of R. All parameters are calibrated in advance.

- Gap-Approaching-Signal: To approach the gap, a bi-directional ACC is proposed to coordinate the relative position of R with P_l and P_f. The detailed formulation is as follows.

$$\bar{u}_R^{P_l}(t + \Delta t) = \left(\frac{1}{h_{dl}}\right) * (\psi_R - \psi_{P_l} - L_d^m + \Delta t * (u_{P_l}(t) - u_r(t))) \tag{85}$$

$$\bar{u}_R^{P_f}(t + \Delta t) = \left(\frac{1}{h_{df}}\right) * (\psi_R - \psi_{P_f} + L_d^m + \Delta t * (u_{P_f}(t) - u_r(t))) \tag{86}$$

$$\bar{u}_R^{approach}(t + \Delta t) = k_R^{P_l} * \bar{u}_R^{P_l}(t + \Delta t) + k_R^{P_f} * \bar{u}_R^{P_f}(t + \Delta t) \tag{87}$$

$$\bar{a}_R^{approach}(t + \Delta t) = (\bar{u}_R^{approach}(t + \Delta t) - u_R(t))/\Delta t \tag{88}$$

where $\bar{u}_R^{approach}(t + \Delta t)$ is the approaching velocity signal for R, $\bar{u}_R^{P_l}$ and $\bar{u}_R^{P_f}$ are respectively the gap-approaching velocity signal component with respect to P_l and P_f, L_d^M is the safety margin consists of vehicle length and a minimum desired merging gap 3.5 m, h_{P_l}, h_{P_f} are the time headways from R to P_l and P_f respectively, $k_R^{P_l}, k_R^{P_f}$ are the weights of two components both set to 0.5 in this research.

The combined car-following and gap-approaching signals are given as follows.

$$\bar{a}_R(t + \Delta t) = min \begin{cases} \bar{a}_R^{approach}(t + \Delta t) \\ \bar{a}_R^{cf}(t + \Delta t) \end{cases} \tag{89}$$

$$\bar{u}_R(t + \Delta t) = u_R(t) + \bar{a}_R(t + \Delta t) * \Delta t \tag{90}$$

4 Connected Vehicle-based Traffic Sensing System

This research assumes CV/AV can detect surrounding vehicles, and the detections data, as well as the status of ego CV/AVs, can be sent to the roadside control center via CV-V2I communication. Meanwhile, some fixed roadside detectors which are connected to the roadside control center can also detect the vehicle status. The scheme of the detection system is shown in Figure 7.
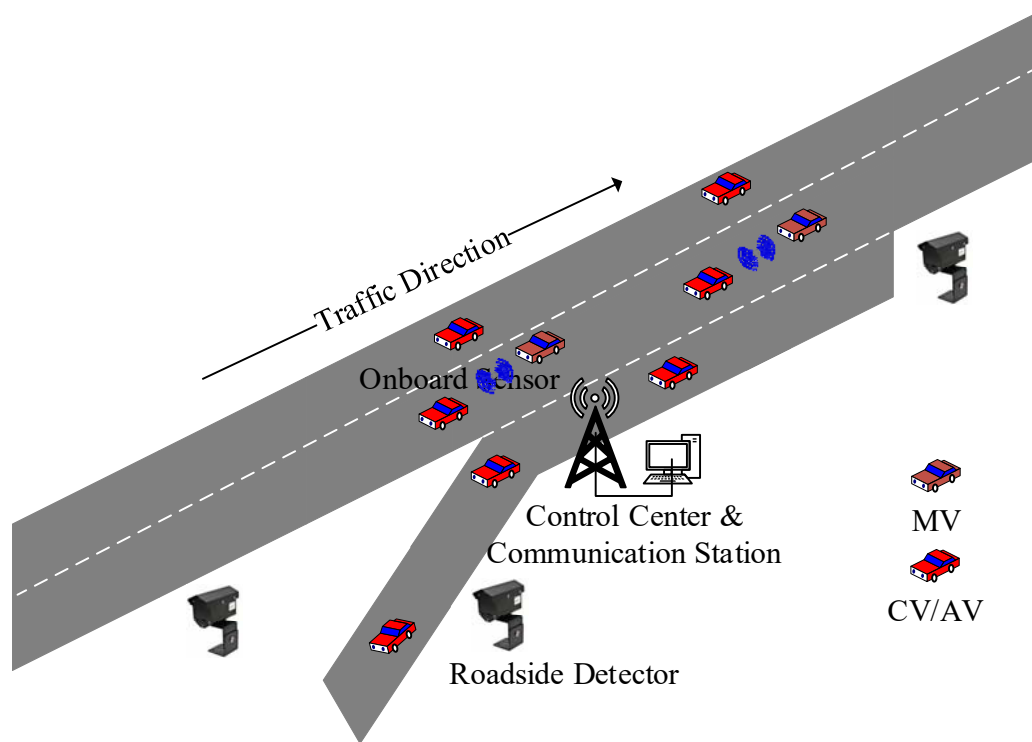
Figure 7 Scheme of CV-V2I Traffic Detection System

The roadside sensors are primarily high-angle traffic monitoring cameras which are widely used in microscopic vehicle trajectory detection projects such as Next Generation Simulation (NGSIM). They can precisely capture the vehicles' status in a fixed location. Meanwhile, the CV/AV's onboard range sensors serve as a mobile sensing system to

capture their surrounding traffic. Thus, this integration sensing system can support the proposed DMA methods by creating the lane speed profiles presented in equation (56).

4.1 Traffic Detection from Roadside Fixed Sensors

Similar to the cameras applied in NGSIM, the roadside fixed sensors can provide the detailed trajectories of all vehicles in the covered area. The trajectory data shall minimally include the following entries to generate ISP:

- Time Stamp: The current system time

- Current Speed: The speed of a vehicle at the current instance

- Current Longitudinal Location: The vehicle's current location from the start of the link. It's presented as "LocalY" in NGSIM, and it's also the same with the linear referencing coordination ψ mention in chapter 3.3, equation (55).

- Current Latitudinal Location: The vehicle's current location from the left-most boundary of the currently occupied road. The latitudinal location can indicate in which lane the vehicle is occupying.

4.2 Traffic Detection from Onboard Range Sensor

This research assumes the onboard range sensors are primarily radar and LiDAR. The detection content of both radars and LiDAR can be abstractly summarized as a set of points represented by their relative distance and angles away from the sensor position. Thus, the relative location and speed can be easily calculated by the detection data. Usually, a LiDAR can cover a 360-degree area surrounding the vehicle, while radars cover a relatively narrow sector. In order to represent a most common sensor scenario, this research assumes that the vehicle is equipped with four abstract range sensors which provide coverage similar to

LiDAR and radar but keep some blind-zones left. The detection result of these range sensors is distance and angles of virtual LiDAR/Radar beams casting from the ego CV/AV. This research does not consider object segmentation and object detection issue. In another word, the content only consists of the detection of vehicles regardless of static infrastructures (e.g., walls, trees, etc.) and pedestrians. At the same time, the different vehicle objects are already classified in the detection content.

Figure 8 shows the example of the vehicle detection range and the conveyed information for a detected object. The areas indicated by white lines in Figure 8a (left half) shows the detection of surrounding vehicles. The black line between V_4 and V_7 represent the center-to-center relative position estimated by reflection information of range sensor beams. The areas indicated by red lines in Figure 8b (right half) shows the overall detection range of all four types of range sensors equipped onboard.
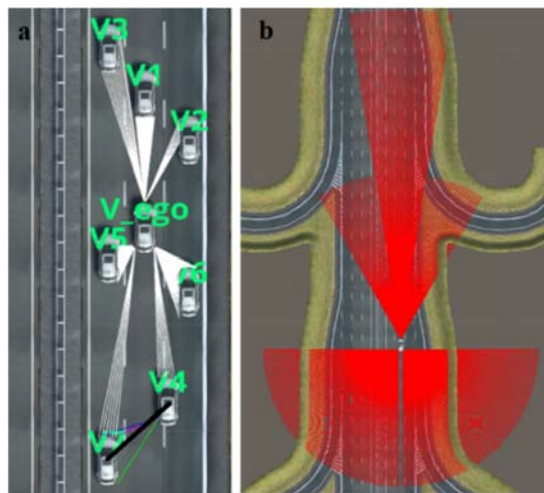
(a) Detected Vehicles (b) Total Detection Range

Figure 8 Scheme of Vehicle Detection by Onboard Range Sensors

The detection information c_i of vehicle V_i consists of the detailed sensor data, i.e., a set of angles θ and distances ρ of range sensor beams which are reflected by V_i. The reflection information of k_{th} range sensor beam reflected by V_i can be easily converted to a 2-D relative position vector $b_{i,k}$, while the height-axis is fixed and ignored in this paper:

$$b_{i,k} = (x_{i,k}, y_{i,k}) = \left(\rho_{i,k} \cos \theta_{i,k}, \rho_{i,k} \sin \theta_{i,k}\right) \tag{91}$$

$$b_{i,k} \in c_i, c_i \in \mathbb{C}_{ego/sender}$$

Assuming a CV/AV noted as V_{ego}, its detection set can be represented as $\mathbb{D}_{ego}$.

$$\mathbb{D}_{ego} = \left\{ d_i \middle| d_i = (x_i, y_i), i \in \mathbb{I}_n^{ego} \right\} \tag{92}$$

The center-to-center relative position d_i of any vehicle V_i from V_{ego} as described in equation (92) can be estimated by the information of range sensor beams b_i reflected by V_i as described in equation (91).

As shown in Figure 8a, this research assumes that an object can be detected by four types of range sensors: two forward range sensors (forward long-range sensor and forward short-range sensor) and two side-rear range sensors (left-rear range sensor or right-rear range sensor). The estimation method for objects detected by a different range of sensor types varies as discussed below.

(1) Forward Range sensor Detection:

As shown in Figure 8a, V_1, V_2, V_3 are in front of V_{ego} within a sector range with a radius ρ_{fwd} and angle $\left[-\theta_{fwd}, +\theta_{fwd}\right]$. They represent three possible conditions of range sensor

beams reflection respectively: 1) only reflected by the rear end; 2) only reflected by side; 3) reflected by both rear-end and side. The condition can be clarified by checking the relative coordinates of the longest and shortest reflected range sensor beams. Their relative position vector d_1, d_2, d_3 from V_{ego} can be estimated by reflection position vectors $b_{i,k}$ of range sensor beams as:

$$d_1 = \left\{ \left(x_{1,k_0}, y_{1,k_0} + 0.5\tilde{l} \right) \mid \left(x_{1,k_0}, y_{1,k_0} \right) = \text{arg}min\left(\rho_{1,k} \right) \right\} \tag{93}$$

$$d_2 = \left\{ \left(x_{2,k_0} + 0.5 * \tilde{w} * (-1)^s, y_{2,k_0} \right) \mid \left(x_{2,k_0}, y_{2,k_0} \right) = \left(arg\ min\left(\rho_{2,k} \right) + \right. \right.$$

$$\left. arg\ max\left(\rho_{2,k} \right) \right) / 2 \right\} \tag{94}$$

$$d_3 = \left\{ \left(x_{3,k_0} + 0.5 * \tilde{w} * (-1)^s, y_{3,k_0} + 0.5\tilde{l} \right) \mid \left(x_{3,k_0}, y_{3,k_0} \right) = \text{arg}min\left(\rho_{3,k} \right) \right\} \tag{95}$$

In which, $b_{i,k} = \left(x_{i,k}, y_{i,k} \right), b_{i,k} \in b_i \in \mathbb{B}_i$ is the relative position vector of the k_{th} reflected range sensor beam from the target vehicle V_i as discussed in eq. (91). $\tilde{l} = 4.7\ meters$ is the assumed vehicle length, and $\tilde{w} = 1.85\ meters$ is the assumed vehicle width. The note s in eq. (94)(95) indicates that the range sensor beam shots at the left side of V_i when $s = 0$ or right side when $s = 1$.

(2) Side Rear Range Sensor Detection

As shown in Figure 8a, V_4, V_5, V_6 are detected by the side-rear range sensors. They represent three range sensor beams reflection conditions respectively: 1) only reflected by front end; 2) only reflected by side; 3) reflected by both front end and side. Their centre-to-centre relative position vector from V_{ego} can be estimated as:

$$d_4 = \left\{ \left(x_{4,k_0}, y_{4,k_0} - 0.5\tilde{l} \right) \mid \left(x_{4,k_0}, y_{4,k_0} \right) = \left(\text{arg}min\left(\rho_{4,k} \right) + argmax\left(\rho_{4,k} \right) \right) / 2 \right\} \tag{96}$$

$$d_5 = \left\{ \left(x_{5,k_0} + 0.5 * \widetilde{w} * (-1)^s, y_{5,k_0} \right) \mid \left(x_{5,k_0}, y_{5,k_0} \right) = \left(\mathrm{arg}min(\rho_{5,k}) + \right.\right.$$

$$\left.\left. \mathrm{arg}max(\rho_{5,k}) \right) / 2 \right\} \tag{97}$$

$$d_6 = \left\{ \left(x_{6,k_0} + 0.5 * \widetilde{w} * (-1)^s, y_{6,k_0} - 0.5\widetilde{l} \right) \mid \left(x_{6,k_0}, y_{6,k_0} \right) = \left(\mathrm{arg}min(\rho_{6,k})^{1-s} + \right.\right.$$

$$\left.\left. \mathrm{arg}max(\rho_{6,k})^{s} \right) \right\} \tag{98}$$

In which, the note s indicates that the target vehicle is detected by the right-rear range sensor when $s = 0$ or left-rear range sensor when $s = 1$.
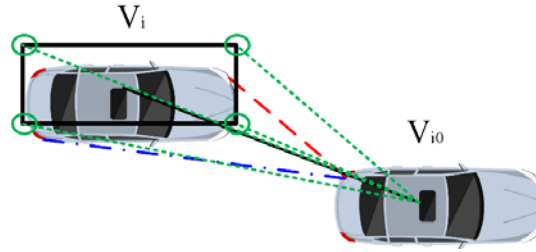
Figure 9 Scheme of Relative Position Estimation based on Range Detector Data

Figure 9 shows the position estimation scheme. Green dot lines are the boundary of range detector beams reflected by objects, red dot line is the shortest distance, blue dot line is the longest distance, and the black line is the estimated relative position vector. Thus, the estimated location of the detected car can be calculated by the relative position vector and ego car's GPS location.

4.3 Existing Methods of Vehicle Localization and Identification

Most of the related research efforts have been made towards the vehicular localization issue in the CV environment. It's a common idea to use their position to identify and track the

vehicles. Among the localization technologies, the most popular one, GPS, is widely equipped and utilized in daily traffic operation.

Some research has been conducted to improve GPS accuracy for vehicle tracking. Fujii *et al.*(Fujii et al., 2011) have proposed a method which uses GPS position and relative position information measured by range sensors to get a more accurate vehicle position with a mathematical likelihood estimation model. This method can also localize the surrounding vehicles which cannot participate in the system. Choi, Hur, and Seo (Choi, Hur, & Seo, 2014) have proposed a method to improve the localization accuracy by matching the topology of local vehicle map which is generated by GPS location and range sensor detection. Similarly, Rohani, Gingras, and Gruyer (Rohani, Gingras, & Gruyer, 2014), Sakr, Bansal (Sakr & Bansal, 2016), and Rauch *et al.*(Rauch, Maier, Klanner, & Dietmayer, 2013) have also respectively contributed to the cooperative map matching methods using GPS and range sensor detection. Yuan *et al*. (Yuan, Krishnan, Chen, et al., 2017; Yuan, Krishnan, Duraisamy, Maile, & Schwarz, 2017) proposed a track-to-track association method to identify the sender by matching the track obtained from GPS information of the message sender to a set of tracks obtained from receiver's onboard ranging sensors. They also applied Kalman filters to reduce the effect of GPS errors. These methods can remarkably improve the accuracy of localization based on low-cost GPS and range sensor data. However, these methods only aim at the positioning problem but regardless of the question that which vehicle is actually the sender who transmits the position information in CV network, which will be a difficult problem when the GPS is highly biased or lost.

Some other research efforts have been made while considering not to use GPS position. Saiprasert and Thajchayapong (Saiprasert & Thajchayapong, 2015) have proposed a method to identify the vehicles by their dynamics (i.e., acceleration) detected by range sensor and received in CV messages. Fujita *et al.*(Fujita, Yamaguchi, Higashino, & Takai, 2016) proposed a method which utilizes the velocity information. These methods require additional detection of vehicles' dynamic features, which lead to a higher risk in efficiency and accuracy than those which require only positioning information. These methods also have limitations when the detected kinetic features of surrounding vehicles are remarkably similar, especially in stable traffic (free flow or congested) or when there are not enough time-series kinetic data to find a unique driving pattern.

4.4 Simulation Modeling for V2I-based Onboard Vehicle Detection

The proposed CV-V2I vehicle detection method is implemented and validated in a simulation environment powered by Unity3D engine. The simulation environment enables the analysis of real 3-D geometry relationship between vehicles on the road, and it also provides features to simulate vehicle operation and sensor detection.

Figure 10 Scheme of Simulation Environment

The experiment conducted in the Unity3D simulation environment is designed to validate the performance of the CVV2I vehicle detection for the vehicles in the same lane as well as adjacent lanes. Thus, a 3-lane straight highway segment is built in simulation as shown in Figure 10. Realistic traffic flow is configured where all simulated vehicles will match their trajectory records obtained from ground truth dataset or VISSIM traffic simulation. The green numbers attached to the car in the simulation scene indicate their unique ID.

4.5 Simulation Results on CV-V2I Vehicle Detection and Relative Position Estimation

An experiment study is conducted in the simulation environment to analyze the performance of the relative position estimation method proposed in section 3.4.1. The simulation environment is built as described in section 4.2.

In the experiment, every vehicle checks the estimated relative position of all other detectable vehicles and their actual position in each simulation step, and then a numerical analysis is conducted to evaluate the error of position estimation. The results are shown in Figure 11 and Table 3.

Table 3 Error of Relative Position Estimation (meters)

Statistic of Absolute Values	Error of Relative Position	Error of Relative Position Norm
Maximum	4.54	4.29
Minimum	0.01	0
Mean	0.81	0.45
STD.	0.95	0.94
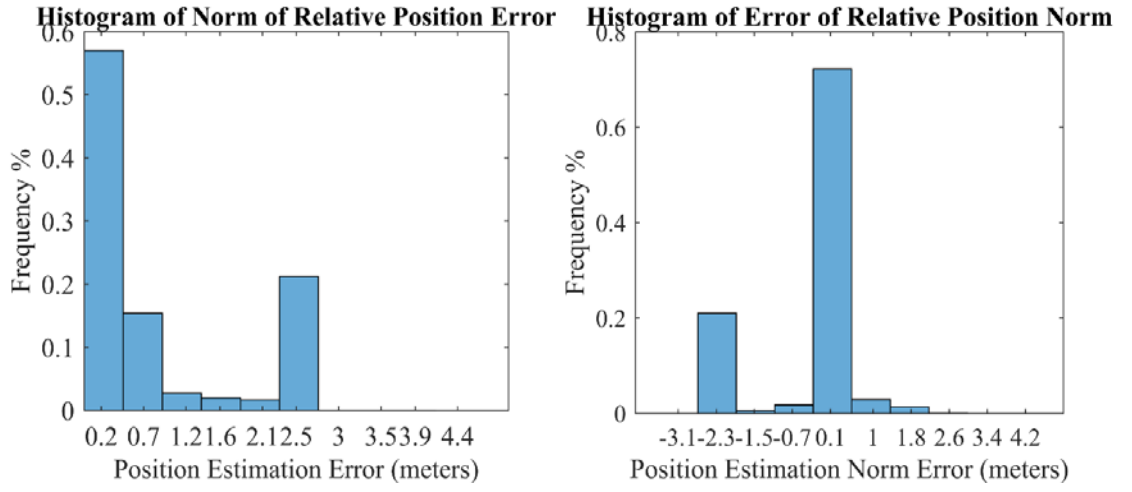
(a) The norm of Relative Position Error (b) Error of Norm of Relative Position

Figure 11 Histogram of Errors between the Estimation and the Truth of Relative Positions

The error of relative position shown in the first column in Table 3 and Figure 11a is calculated as:

$$e_1 = \|\hat{d} - d\| \tag{99}$$

While the error of relative position norm in the second column in Table 1 and Fig.4a is calculated as:

$$e_2 = \|\hat{d}\| - \|d\| \tag{100}$$

e_1 is applied to evaluate the value of position estimation error, and e_2 is applied to evaluate the bias of position estimation error. The statistic results indicate that the maximum error of position estimation is about 4.54 meters which is about the assumed length of a vehicle.

5 Simulation Modeling and Experimental Design

5.1 Site description and simulation network design

The proposed method is evaluated with VISSIM traffic simulation. A baseline VISSIM model is built and calibrated the 2-hour ground truth data collected at IH-35 in Austin, Texas. As illustrated in Figure 12, There is a speed limit of 60 MPH on mainline, and 40 MPH on-ramp attached to the IH-35 frontage road and the corridor has heavy traffic in morning peak hours due to the commuting traffic coupled with heavy freight traffic in the U.S. The area near the end of the corridor segment has a combination of vertical and horizontal curves that can trigger bottlenecks in addition to the downtown traffic downstream across the river. One weaving section is selected as the experiment site to simulate the proposed control strategy. The weaving section is near Woodland Avenue which is shown in Figure 12.
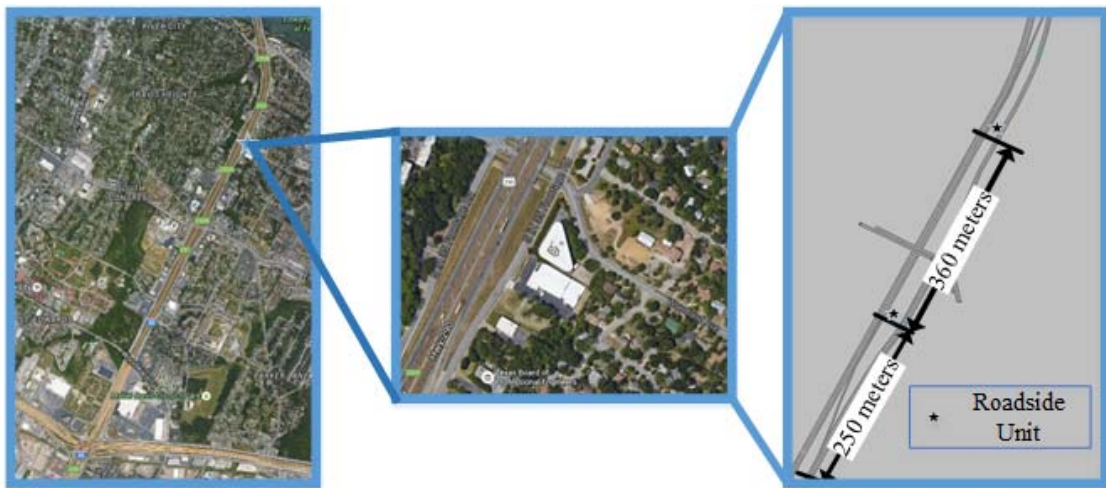
(a) Satellite view of the test site
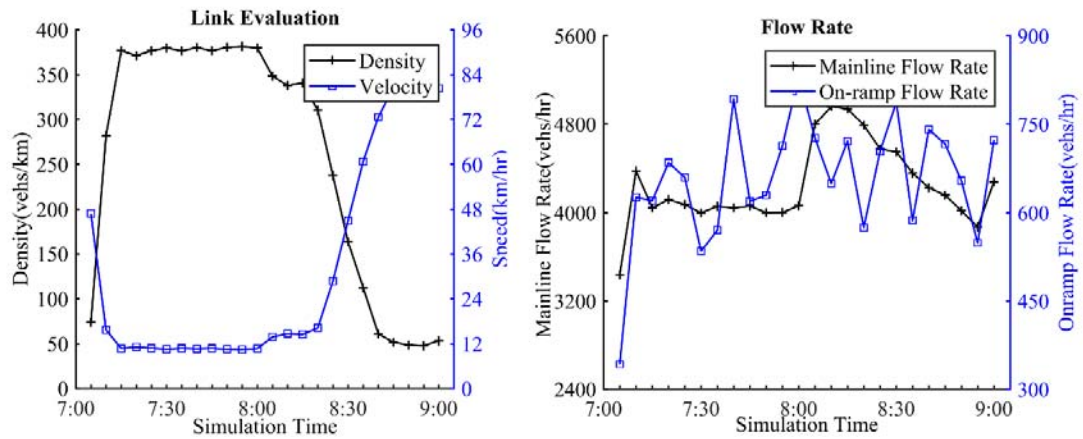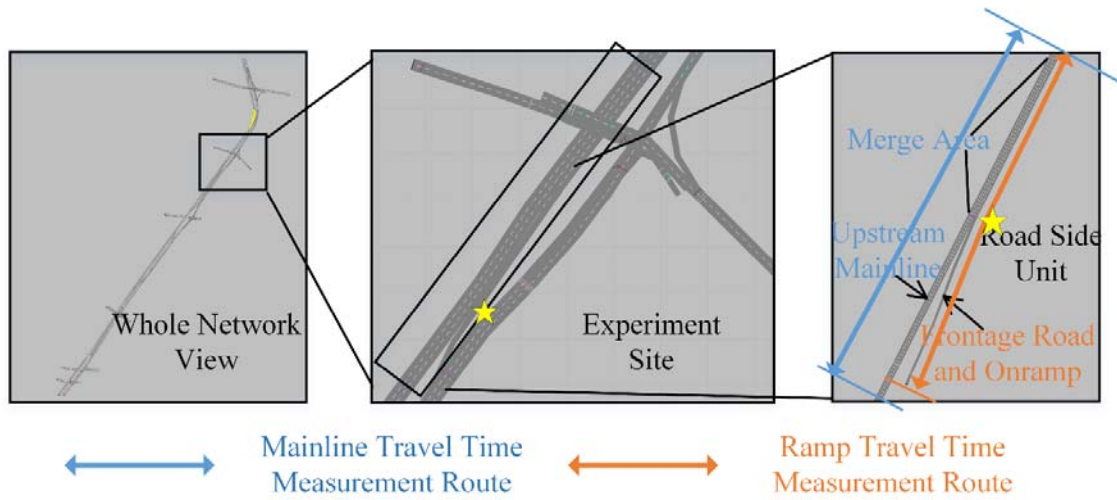
(b) VISSIM view and baseline traffic profile.

Figure 12 Experiment site and baseline traffic profile.

(Oltorf St. Weaving Section at IH-35 corridor, Austin, TX, USA).

I assume the roadside unit (RSU) is set at the junction of the on-ramp and mainline which is also the start of the acceleration lane. The communication radius is about 350 meters which can cover the whole merge area, the on-ramp and a part of upstream mainline. The proposed model is implemented by a VISSIM's Application Programming Interface (API)

named External Driver Model (EDM). The simulation step is 0.1 second which is also the time interval for information update. The CV is assumed to have an additional perception-reaction time. The parameters of the simulation are shown in Table 4.

Table 4 Configuration for VISSIM simulation

VISSIM Simulation		VISSIM Simulation	
Desired Speed on Mainline (km/h)	95	Relative Flow of HGV (%)	10.5
Desired Speed on Ramp (km/h)	65	Simulation Runs	25
Simulation Period (s)	7200	Simulation Step (s)	0.1
Relative Flow of Car (%)	89.5	Perception-Reaction Time (s)	1
Gipps Model		**ACC Model**	
Max Acceleration (m/s^2)	4.89	k_0	2.35
Max Deceleration (m/s^2)	-1.82	k_1	1.30
Assumed Max Deceleration of Preceding Car (m/s^2)	-2.10	k_2	0.42
Desired Speed (m/s)	26.22		
Safe Distance (m)	1.21		

VISSIM configuration has been calibrated so that the discrepancy between simulated and observed flow data at the I-35 corridor is less than 10%. The parameters for Gipps model have been calibrated in advance according to the original microscopic simulation traffic data including vehicle trajectories(Peter J Jin, Yang, & Ran, 2014). Performance measures considered in this study 1) travel time of onramp vehicles and mainline vehicles throughout the weaving section; 2) the minimum time to collision (TTC) during lane changing. TTC will be counted only when the velocity of the merging vehicle is slower than the following mainline vehicle. The performance during the whole period as well as the performance during congestion will be both analyzed.

5.2 Simulation Model Building and Calibration

To ensure the baseline model is consistent with the field data, a VISSIM simulation model is built and calibrated based on the field traffic flow data. We configure the entry rate, desired speed, and path split rate in simulation to make the flow rates in mainline and ramp

close to the observed field data. As shown in Figure 13, the discrepancy between the simulated flow rate and observed flow data is less than 10%.
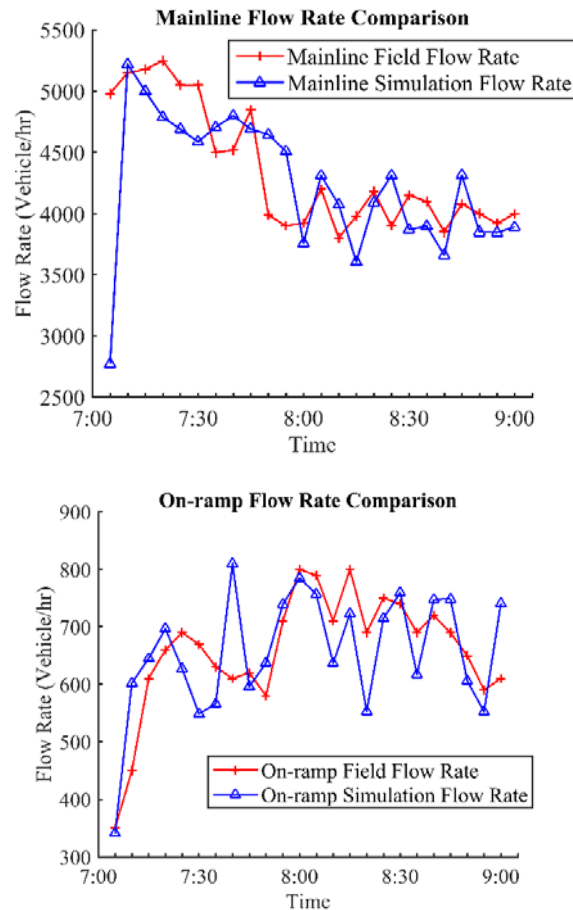
Figure 13 Comparison of field flow rate and simulation flow rate

5.3 Simulation Performance Measurements

Performance measurements considered in this study 1) travel time of onramp vehicles and mainline vehicles throughout the weaving section; 2) the time to collision (TTC) during lane changing. In the travel time evaluation, all vehicles passing through the merging area are considered. The measured path for on-ramp vehicles includes the entry frontage road and the acceleration lane. The measured path for mainline vehicles includes the mainline merging link and its upstream link.
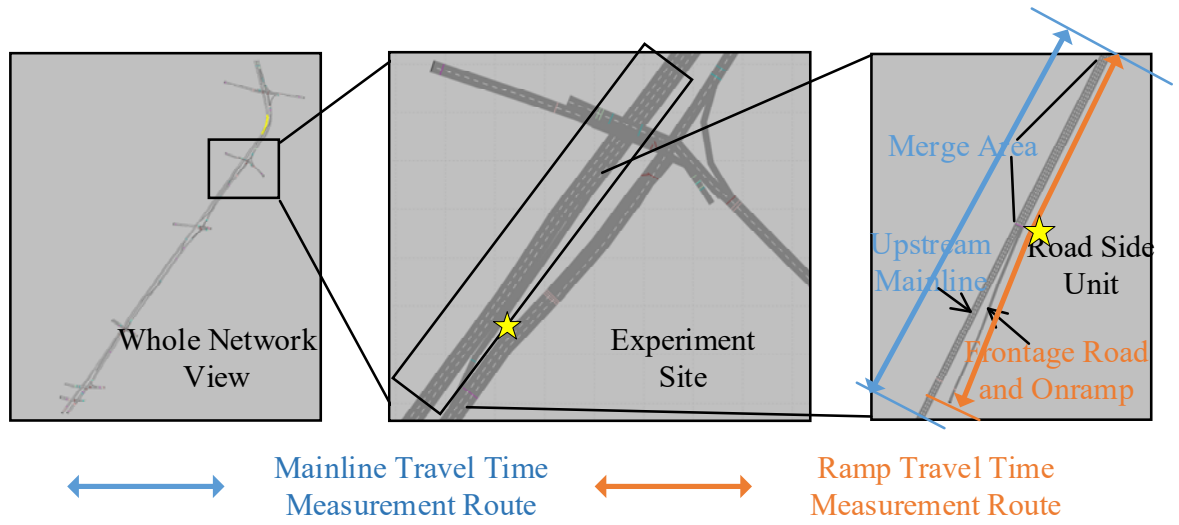
Figure 14 Travel Time Measurement Route

TTC is counted only when the velocity of the merging vehicle is slower than the following mainline vehicle. The following equation is applied to calculate TTC:

$$TTC = \frac{\psi_{P_r} - \psi_{P_l}}{u_{P_r} - u_{P_l}} \qquad (101)$$

In TTC evaluation, we only calculate the TTC between the mainline lagging vehicle and on-ramp vehicle during the merging process because only these vehicles are under controlled and their TTCs are changed by our model.

The performance during the whole period as well as the performance during congestion is analyzed. Two representative DMA algorithms from Park et al.'s and Davis et al.'s works are also implemented for the model comparison.

5.4 Reference models and mixed-control implementation

In the evaluation study, Park et al.'s CV-based model(Hayat et al., 2014; Park et al., 2011) and Davis' AV-based model(Davis, 2007) are selected and implemented as the reference models. Park et al.'s model is a representative CV-based method with field validation.

Davis model employs ACC control, and it considers the use of AV functionalities in DMA algorithms. I implemented Park et al.(Hayat et al., 2014; Park et al., 2011)'s model in VISSIM external driver model in the same simulation network. The vehicles are randomly categorized as "compliant" and "non-compliant" to the control signal. I evaluate three scenarios including low compliance rate 25%, medium compliance rate 60% and full compliance rate 100%. Although Park et al.(Park et al., 2011) announced that their model only works with 60% compliant vehicle or more, the performance with a lower compliance rate is still analyzed. Davis model is also implemented in VISSIM external driver model. The scenarios with 25%, 60%, and 100% CAV penetration rate are evaluated. I assume that MV can be detected precisely through roadside sensors, but only AVs are under DMA control.

6   Evaluation results & discussion

A simulation study is conducted to implement the proposed DMA model. Scenarios with different compliance rate are simulated for each. 25% compliance rate is employed to reflect the low penetration rate situation, 60% is employed for medium penetration rate situation, and 100% reflects the perfect deployment situation.

6.1 Merging trajectory validation of the V2I-Mixed DMA model

Figure 15 shows six sets of sample trajectories for different merging scenarios. The x-axis indicates the simulation time; while the y-axis represents the locations of vehicles from the start of the merging segment. Dash lines indicate the boundaries of the acceleration lane. The blue circle indicates the time and location at which the paring is confirmed. The red square indicates the time and location of the lane change that completes the merging. Several representative vehicle trajectory combinations are presented in Figure 15.

Figure 15a and Figure 15b show the early-merge and late-merge scenarios respectively. The red circle shows the time and location of the final pairing and the red square indicates the lane-change event that completes the merging. Blue lines are the trajectories of PL and PF; while the red line is the trajectory of R. In Figure 15a, the ahead merge vehicle arrives at a relatively higher speed than PL and PF and adjust its speed to smoothly merge into the PL-PF gap. In Figure 15b, vehicle speeds are lower than in Figure 15a. Merging vehicles made lane changes close to the end of the acceleration lane. The proposed algorithms can adapt to different speed conditions of PL and PF and select the appropriate pairing opportunities.

Figure 15c and Figure 15d illustrate the accelerating and decelerating merging scenarios. In those scenarios, there are significant velocity differences between the initial

velocity of ramp vehicles and the mainline traffic stream. The proposed algorithms can also trigger the adjustment of the approaching velocity of ramp vehicles and identify a proper gap opportunity for merging.

Figure 15e and Figure 15f shows a more complicated behavior in which the paring between merging and PL-PF vehicles keeps fluctuating. The system may release one R-PL/PF pair for a new pairing due to the criteria mentioned in the above methodology part. The refreshing process may occur multiple times. In the figures, the dashed line shows the trajectories of all PL/PF combinations that are initially paired with R but eventually unpaired. The blue line shows the trajectories of the PL and PF in the final pairing. Circles denote the timing and location of the final pairing. In Figure 15e, the merging vehicle eventually rejects the gap represented by purple trajectories; while in Figure 15f, the merging vehicle is accelerating through acceleration lane and switched over multiple gaps and eventually settle to the gap illustrated with solid blue lines.

In summary, Figure 15 illustrates the adaptive capability of the proposed algorithm against different merging conditions. This demonstrates that the proposed algorithm actually implemented many of the macroscopic early-merge(Datta et al., 2004), late-merge(Grillo et al., 2008; Kang et al., 2006; Pesti & McCoy, 2001; Pesti et al., 2007), dynamic-merge(Meyer, 2004a), and gap metering(Peter J Jin et al., 2017) characteristics microscopically.
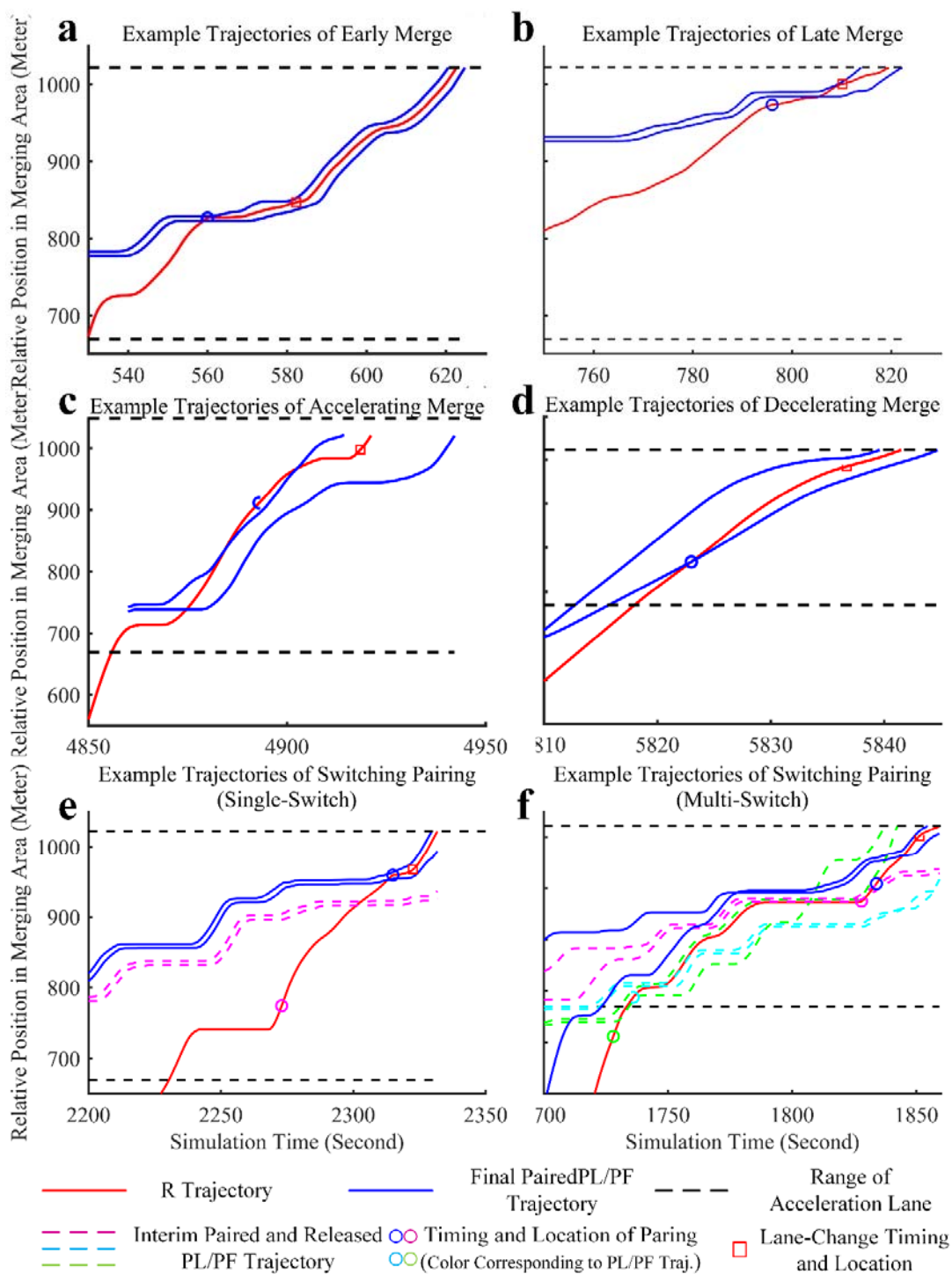
Figure 15 Examples of trajectories of controlled vehicles.

6.2 Spatial Pattern Analysis of Merging Activities
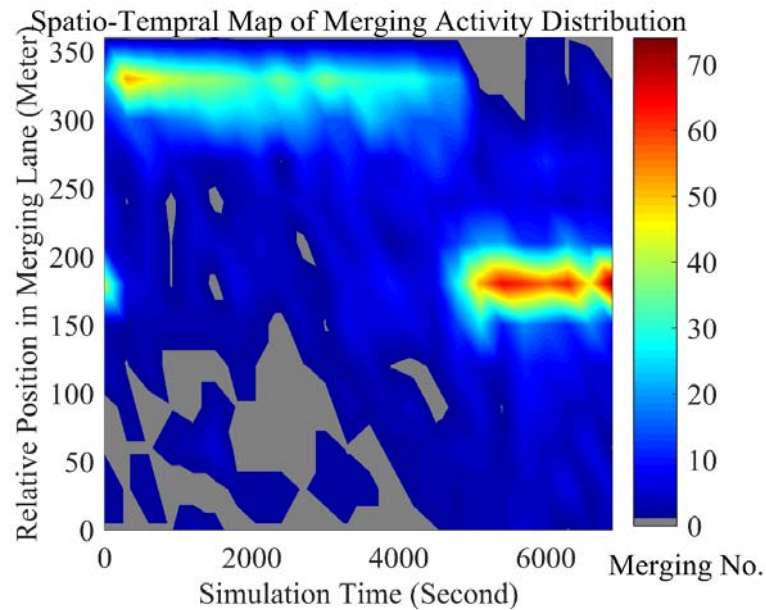
Figure 16 Distribution of merging activities under DMA.

Figure 16 shows the distribution of merging activities. During congestion, the merging activity usually occurs near the end of the acceleration lane. This "Late-Merge" phenomenon indicates that the model takes advantage of the full length of acceleration lane to maximize throughput. During free-flow, the merging activities often occur closer to the beginning of the acceleration lane. This "Early-Merge" phenomenon indicates that the model can promote safe early merging activities during high-speed conditions. Furthermore, the conventional "Dynamic Merge" control schemes are adaptively fulfilled by the proposed algorithm.

6.3 Traffic Conflict Analysis

Meanwhile, the statistical analysis of safety performance is illustrated in Figure 17. The critical distance is defined as the gap size between PF and R when the lane-changing starts, and Time-to-collision (TTC) is calculated by:

$$TTC = \frac{\psi_{p_f} - \psi_R}{v_{p_f} - v_R} \tag{102}$$

The results show that:

1) Park model does not obviously influence TTC because it does not control the vehicle velocity. In contrast, the critical distance is increased, which indicates that this model successfully let mainline vehicle yield to merging vehicle with a larger gap.

2) Davis model tends to take over vehicle control and squeeze the TTC and critical distance distribution to a fixed numerical zone. The peak of the distribution is sensitive to the parameter applied to the control model. The improvement in mobility by this model may be at the cost of a deterioration in safety. In high penetration situation, the small TTC may not be an issue due to the well-configured automated driving. However, it may cause some problems in low penetration rate situation.

3) The proposed V2I-Mixed DMA model has a smoother distribution due to the one-on-one coordinated control during the whole process. The vehicles may have more time to adjust their velocity. However, the distribution is also changed with the parameters such as desired gap length and ACC factors applied in the control model. The calibration and sensitivity analysis of the parameters will be one of the future works.
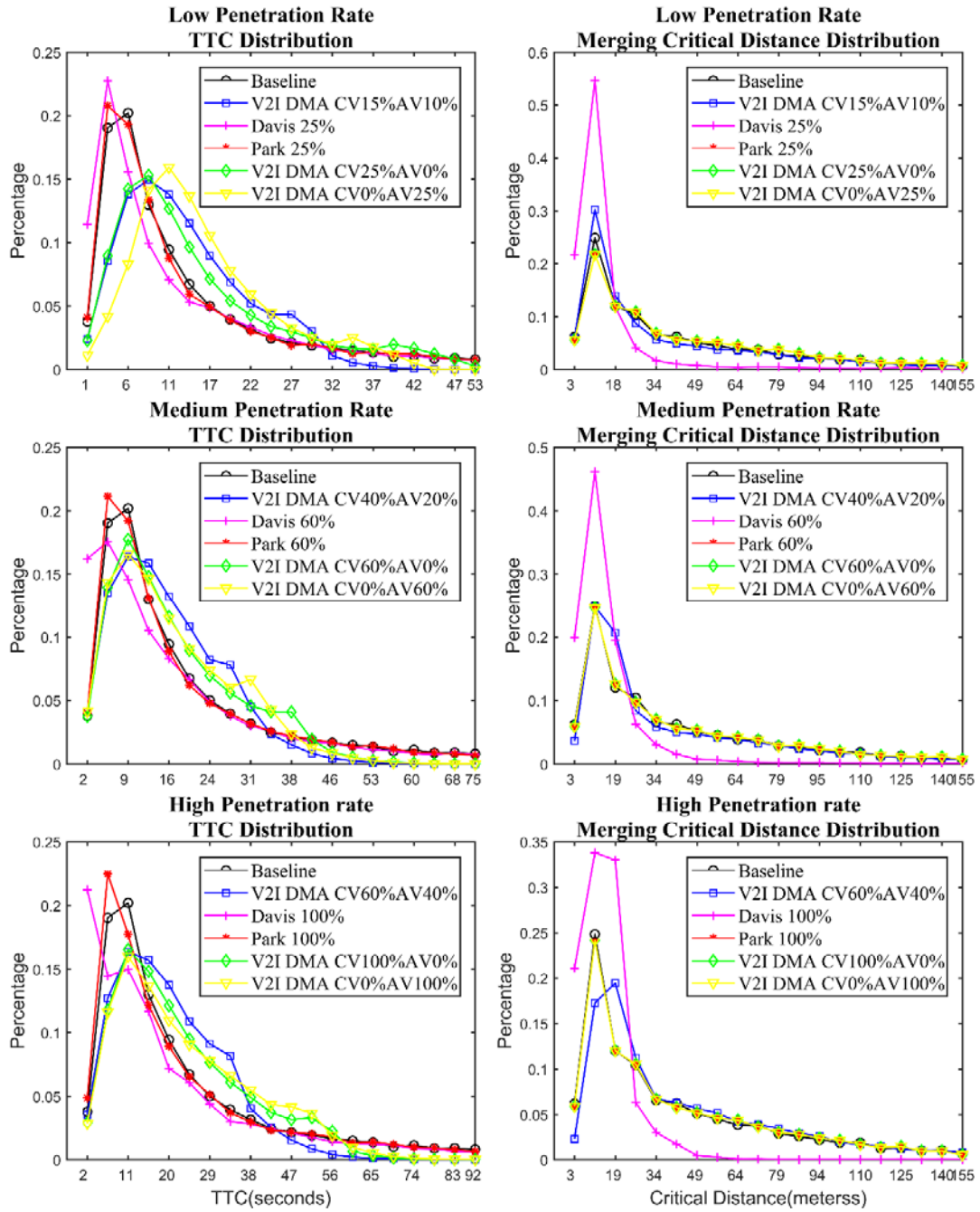
Figure 17 TTC and gap-size distribution (total 25-runs) for comparison models.

In total, 25 different runs of simulation with stochastic traffic condition are conducted. The distribution analysis is based on the average value of all runs. Then, a statistical analysis

of all the results is conducted to represents how the proposed method performs in different simulation environments.

Table 5 Statistical Analysis for Merging Conflicts in 25-runs (CV-AV-MV Mixed)

Eva. Pene.	Average TTC				Average Merging Critical Distance			
	All Period		Peak		All Period		Peak	
	Mean	STD.	Mean	STD.	Mean	STD.	Mean	STD.
Low	27.2	2.8	33.6	2.5	37.2	9.8	18.5	3.4
Medium	32.5	2.8	35.2	2.6	38.7	9.9	20.1	5.6
High	33.5	2.7	39.1	2.6	42.9	9.1	25.3	5.2

6.4 Speed Contour Map Evaluation

Figure 18 illustrates the speed distribution in contour maps to show the comparison of the mobility performance among the proposed V2I-Mixed DMAV2I-Mixed DMA, Davis' and Park's model. In the figures, black dash lines indicate the boundaries of the acceleration lane at the merge section. The congested area is defined as the spatio-temporal area where the average speed is lower than 35 km/h. Three scenarios with respectively low (25%), medium (60%), and high (100%) market penetration rates are evaluated. For Park model, the penetration refers to the CV penetration. For the Davis model, the penetration rates are the rates of AVs. For the proposed V2I-Mixed DMA model, it refers to the combination of CVs and AVs (CV 15%-AV10%, CV 40%-AV 20%, and CV 60%-AV 40%).

The evaluation results of V2I-Mixed DMA model show that mobility performance improves with the increase of the penetration rate. The congested area on the mainline is shrunk by 1.4% with a low penetration rate, 8.1% with medium penetration rate, and 24.2% with a high penetration rate. The congested space-time area (speed less than 35 km/h) is the contour map reduces by 19.3%, 22.2%, and 35.6%, respectively for the low, medium, and high penetration rates.

Davis model, however, shows expanded congested area on the mainline and ramp along with penetration rate increases; while Park model shows a decreasing but fluctuating trend of improvement. Davis model suffers from deterioration by -23.7%, -16.4%, and -48.7% on mainline and -21.5%, -27.1%, and -34.4% on-ramp in low, medium, and high penetration rate scenario respectively. Although Davis model does have slightly better average conditions during congestion compared with Park and the proposed model. The improvement by Park model is 21.4%, 12.1%, and 0.8% reduction of congested space-time areas on mainline, and 17.3%, 14.4%, and 18.5% on-ramp.

The comparison cross three models indicate that in low penetration rate condition, V2I-Mixed DMA model has a similar performance in traffic improvement as that of Park model with slightly better ramp condition. In medium and high penetration rate conditions, V2I-Mixed DMA outperforms Davis and Park model significantly. The result indicates that all three models can improve the traffic mobility onramp without significant disturbance to the mainline traffic. Davis model has a limitation in off-peak, and the on-ramp improvement with Park model is at the cost of performance loss on mainline.
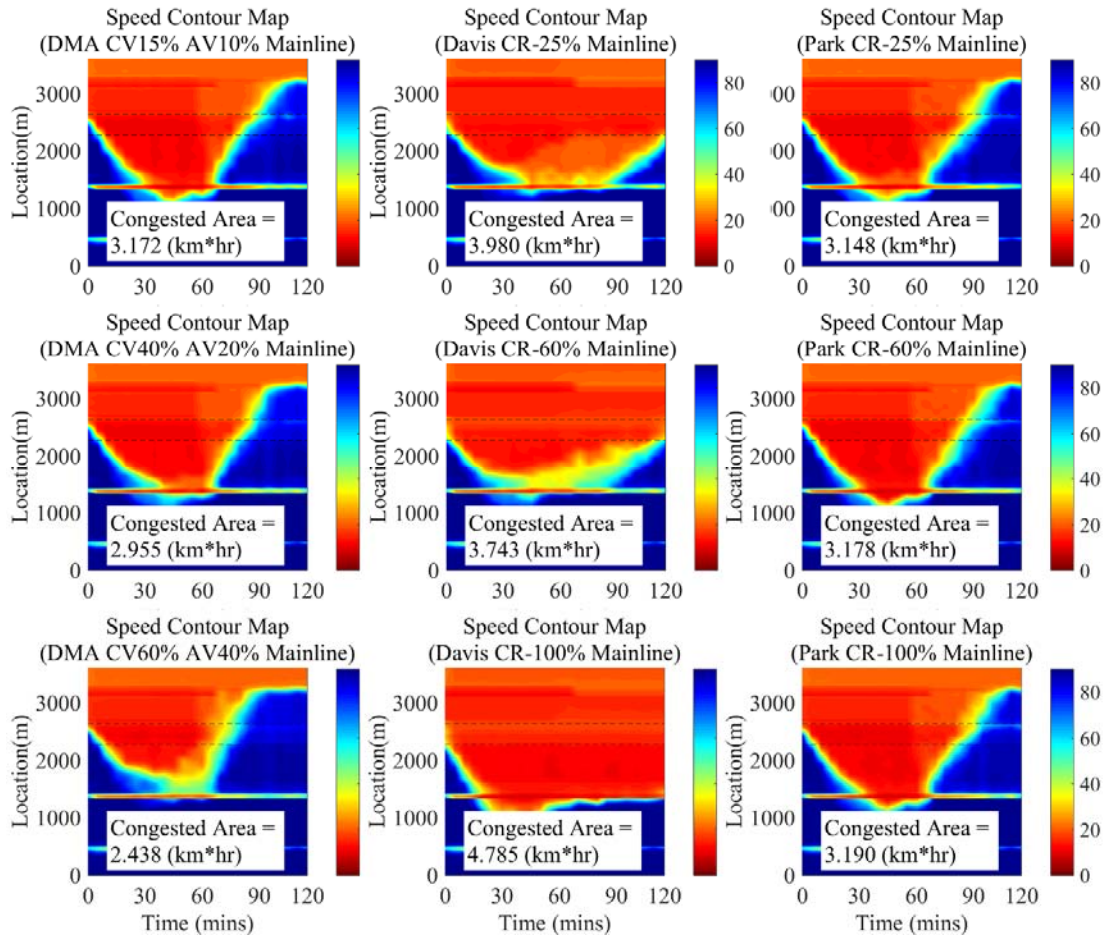
(a) Speed contour map for mainline
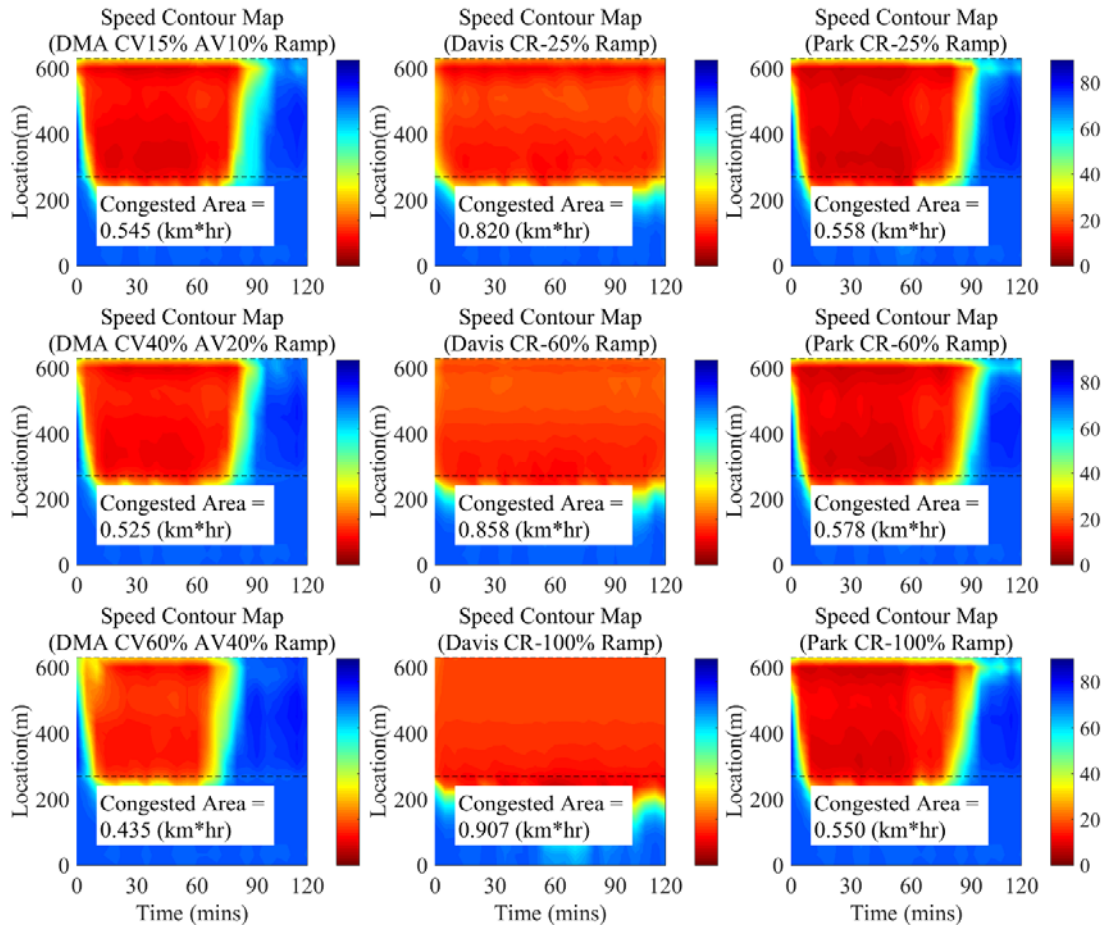
(b) Speed contour map for ramp

Figure 18 Speed distribution comparison.

7 Sensitivity analysis for V2I-Mixed DMA System

I have conducted a 25-run simulation to evaluate the proposed system with different CAV penetration rate combinations. The analyzed penetration rate starts from 5% CV and 5% AV which is a realistic value for current environment(Statista, 2017), and increases to 60% CV and 40% AV which is an ideal situation for decades later. The increasing penetration rate reflects the development and deployment of CAV technologies in real-life traffic currently and years in the future, and apparently, the CV rate will increase faster than AV. I will evaluate Travel Time (T.T.), Link Evaluation, speed contour map, and Time-to-Collision to reflect the performance in mobility and safety. I also compared the results during the entire simulation period and the results during the peak hours.

The general results including travel time, delay time and TTC are shown in **Table** 6. The average travel time and delay are measured based on the routes from the mainline upstream link or the entrance of on-ramp to the end of the merging area as shown in Figure 12. The delay time is defined as the difference between the actual travel time and the free flow travel time. In TTC analysis, I eliminated large TTC's calculated due to the small speed differences.

Table 6 Summary of Sensitivity Analysis on the Impact of Different CV-AV Penetration Rates

Performance Metrics (Average of 25-run)	Baseline		V2I-Mixed DMA CV5%AV5%	
	All period	Peak-hour	All period	Peak-hour
Average travel time(ramp)	114.2	160.9	110.7	152.5
Average travel time(mainline)	123.8	183.2	126.7	183.9
Average delay time (ramp)	83.2	129.9	79.3	121.1
Average delay time (mainline)	99.3	159.1	101.8	159.1

Average of under 85-Percentile TTC	21.2	28.8	22.9	31.3
85-Percentile TTC	83.9	127.9	79.3	101.2

Performance Metrics (Average of 25-run)	V2I-Mixed DMAV2I-Mixed DMA CV15%AV10%		V2I-Mixed DMAV2I-Mixed DMA CV30%AV15%	
	All period	Peak-hour	All period	Peak-hour
Average travel time(ramp)	107.5	145.4	101.1	138.2
Average travel time(mainline)	126.1	183.9	123.2	182.6
Average delay time (ramp)	78.6	113.1	68.6	105.1
Average delay time (mainline)	100.5	158.1	96.9	155.7
Average of under 85-Percentile TTC	27.2	33.6	29.0	36.9
85-Percentile TTC	101.8	101.8	108.7	108.7

Performance Metrics (Average of 25-run)	V2I-Mixed DMAV2I-Mixed DMA CV40%AV20%		V2I-Mixed DMAV2I-Mixed DMA CV60%AV40%	
	All period	Peak-hour	All period	Peak-hour
Average travel time(ramp)	98.9	134.3	84.1	
Average travel time(mainline)	120.8	180.0	109.7	170.6
Average delay time (ramp)	65.9	100.5	50.1	83.1
Average delay time (mainline)	94.1	152.3	81.9	140.6
Average of under 85-Percentile TTC	32.5	35.2	33.5	39.1
85-Percentile TTC	144.8	145.1	147.4	147.4

7.1 Mobility Analysis

The simulation results in **Table** 6 show that the average travel time on mainline increases a little bit when V2I-Mixed DMAV2I-Mixed DMA is applied with a minor penetration rate, and it decreases when more controllable vehicles participate. In contrast, the travel time on ramp does not experience this fluctuation and decrease along with the increase of C/AV penetration rate.

The result of delay time also proves the same conclusion that V2I-Mixed DMAV2I-Mixed DMA can improve the merging traffic positively. The onramp traffic is improved even in low penetration rate situation without significantly disturbing the mainline traffic when only a small proportion of vehicles participate in yielding to merging vehicles. In the high penetration rate situation, both on-ramp and mainline traffic are apparently improved, especially during peak-hour. The overview of delay time for all scenarios is illustrated in Figure 19.
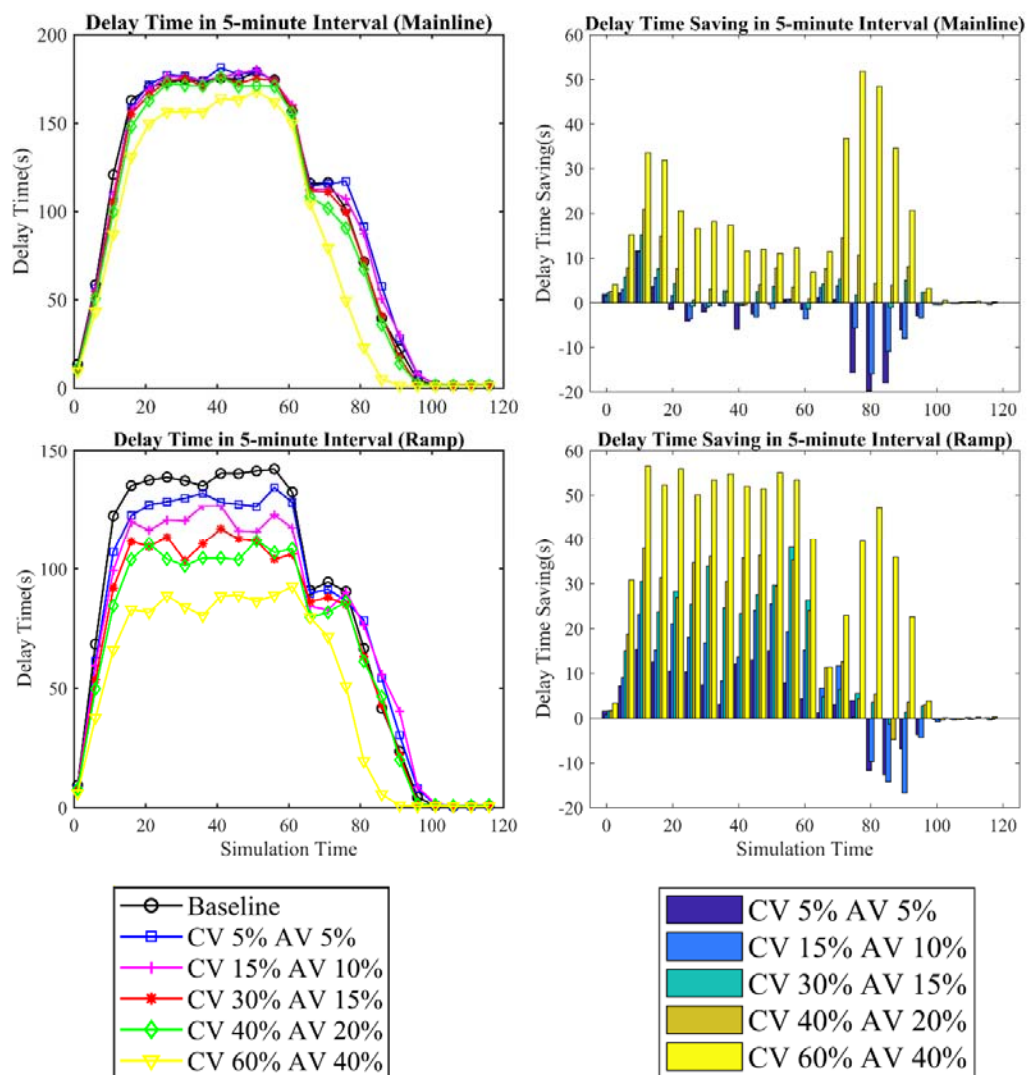
Figure 19 Delay time in 5-minutes intervals for V2I-Mixed DMAV2I-Mixed DMA.

Table 7 Statistical Analysis for Delay Time in 25-runs (CV-AV-MV Mixed)

Eva. \ Pene.	Delay Time				Delay Time Saving			
	Mainline		Ramp		Mainline		Ramp	
	Mean	STD.	Mean	STD.	Mean	STD.	Mean	STD.
Baseline	99.34	7.09	83.17	5.63	0	0	0	0
CV 5% AV 5%	101.81	6.14	79.28	4.67	-2.47	5.47	3.89	5.61
CV 15% AV 10%	100.50	5.39	75.57	6.31	-1.16	7.02	7.60	6.85
CV 30% AV 15%	96.94	4.37	68.60	3.93	2.41	7.35	14.58	7.04
CV 40% AV 20%	94.07	6.09	65.94	5.22	5.27	5.00	17.24	4.63
CV 60% AV 40%	81.89	6.25	50.14	3.94	17.45	6.36	33.03	5.97

An illustration for the traffic speed is also done to reflect the improvement in traffic mobility as shown in Figure 20. The acceleration lane is indicated by black dash lines. I calculate the spatial-temporal area in congestion when the speed is lower than 35 KPH (about 20 MPH). The result shows the congested space-time area is reduced overall, especially on the ramp. Meanwhile, the results also indicate that with higher penetration rate comes better speed amelioration.
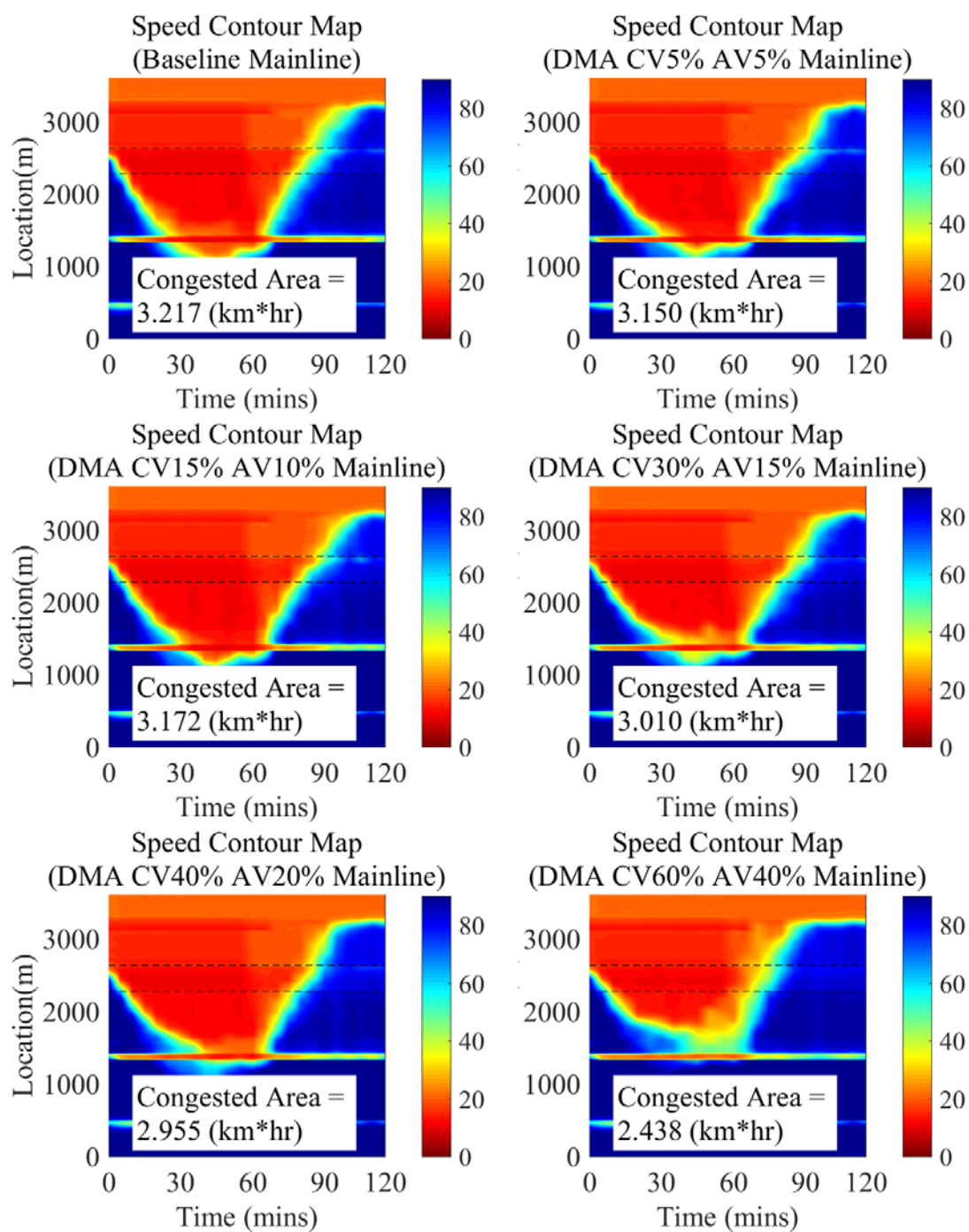
(a) Speed contour map for mainline
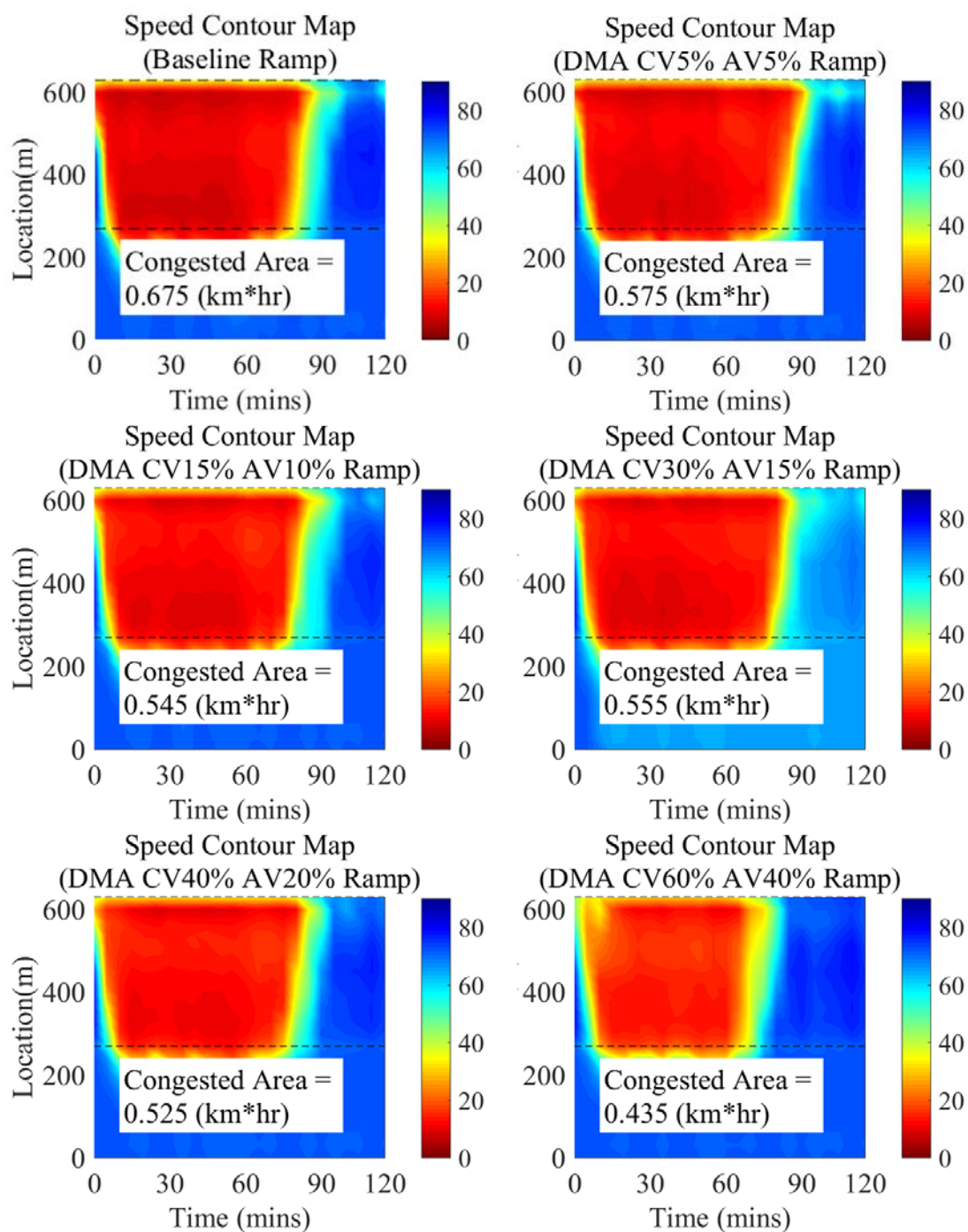
(b) Speed contour map for ramp

Figure 20 Speed contour map for V2I-Mixed V2I-Mixed DMA.

7.2 Safety Analysis

The negative TTC when PF is slower than R is not counted. Results show that PF tends to keep a critical distance away from R when it changes lane, and the critical distance is slightly longer than the usual distance kept by vehicles in the baseline. Meanwhile, the coordinate adjustment for speed between PF and R leads to a larger TTC, which indicates a safer merging activity. The model's performance is generally improved with the increasing penetration rate.
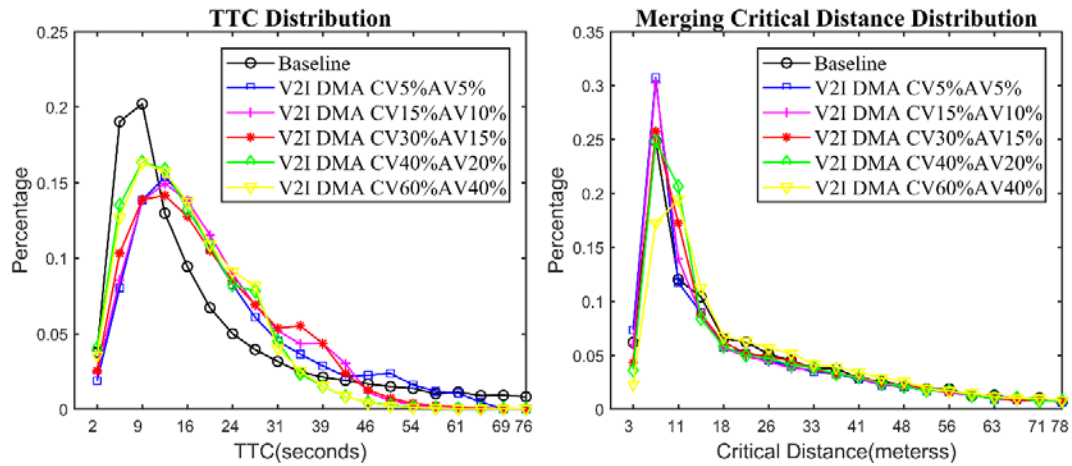
Figure 21 TTC and Merging Gap distribution in merging with V2I-Mixed DMA

7.3 Sensitivity Analysis on Perception-Reaction Time (PRT)

Different level of human perception-reaction time (PRT) is applied in the proposed CV-DMA method to test the impact of different PRT on the model's performance. We choose the PRT from a reasonably small value (0.8 seconds) to a large PRT (4s) which may indicate a distracted driver. The travel time and TTC are evaluated to represent mobility and safety performance.
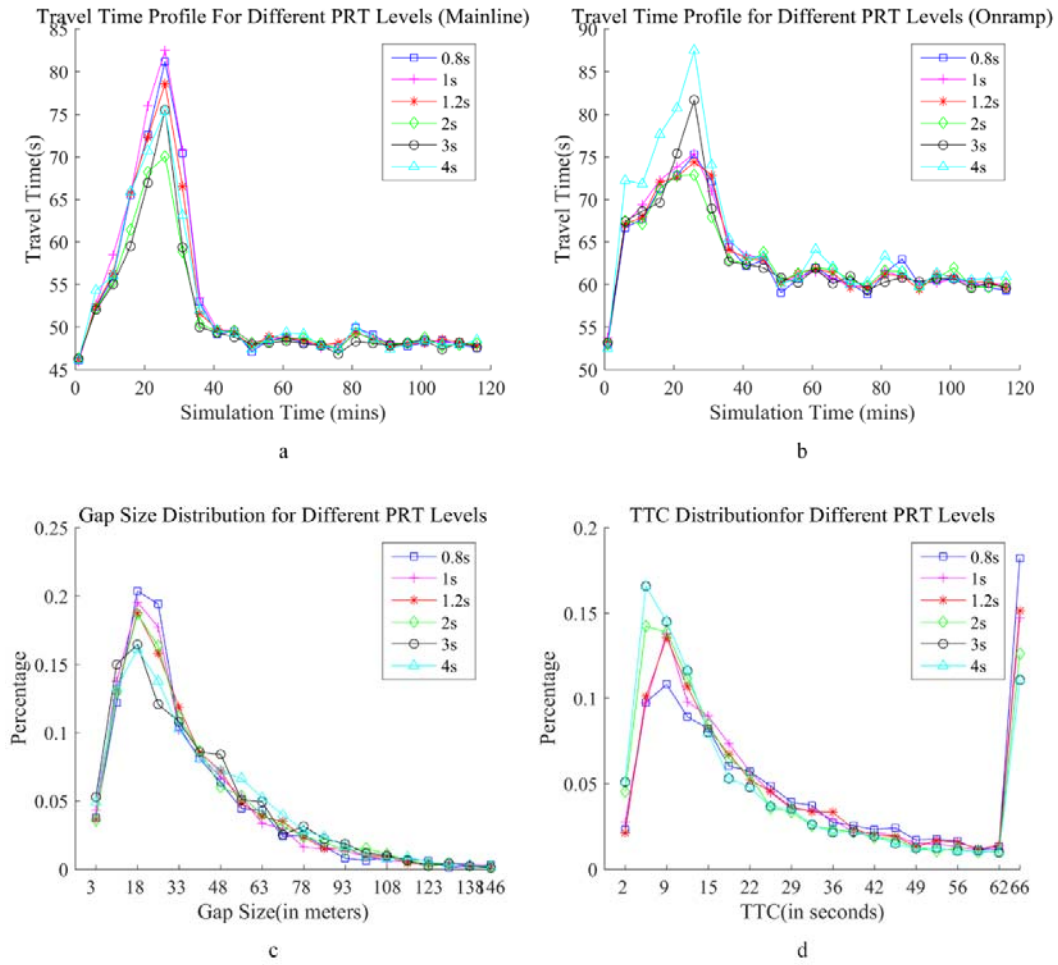
Figure 22 Mobility and safety performance for different perception-reaction time (PRT) levels

8   Conclusion and Future Work

8.1 Summary of Chapters

Chapter 1 introduces the background information of merging conflicts on the highway and some existing solutions. The problem statement, the objectives, and scope of research and research contributions are also presented.

Chapter 2 is a literature review. It includes the overall review of macroscopic merging assistance method and microscopic merging assistance method as well as the detail of some representative microscopic DMA models.

Chapter 3 presents the methodology. The methodology includes three stages: 1) Prediction of instantaneous virtual trajectories based on instantaneous lane speed profiles; the lane speed profiles are generated by CV/AV detection and roadside sensor detection; 2) Vehicle-Gap Pairing based on the IVTs prediction; 3) Gap maintaining and approaching.

Chapter 4 discusses the sensing system which supports the proposed DMA method. The sensing system is integrated with roadside fixed cameras similar to those in NGSIM and CV onboard range sensors.

Chapter 5 discusses the design of a simulation study to validate the proposed method. A unity-based simulation is designed to validate the CV-V2I based vehicle detections, and a VISSIM simulation is designed to test the proposed DMA method. The detail of simulation configuration, calibration, and performance measurement are also presented.

Chapter 6 analyzes the results of the simulation experiment and discusses the performance of the proposed method.

Chapter 7 presents the sensitivity analysis with different CV/AV penetration rate and perception-reaction time. The performance measurements include both mobility performance and safety performance.

8.2 Conclusion Remarks

This research presents a V2I-Mixed DMA method which considers the scenarios with the mixed vehicular environment in highway merge sections. The finds include:

- A CV V2I dynamic merging assistance model considering different types of vehicles (MV, CV, CAV) which have different features in control, sensing, and communication:

  The mixed vehicular environment represents the current state of application and deployment of connected automated vehicle technologies, and it will possibly last for several years more.

- A trajectory prediction algorithm based on the prevailing traffic condition collected by CV V2I traffic sensing system:

  The traffic condition is concluded as lane speed profiles, and the predicted trajectories are presented as instantaneous virtual trajectories.

- A CV-based traffic sensing system which provides support to the proposed DMA system:

  The sensing system consists of a roadside fixed sensor network (i.e., high angle traffic monitoring cameras similar to those in the NGSIM project) and the CV onboard range sensors. A CV-based vehicle detection method and a simulation test

are also proposed to validate that the CV traffic sensing system is feasible and precise enough for lane speed profile generation and IVT prediction.

- A vehicle-gap paring algorithm according to a prediction of their merging potential which comes from the instantaneous virtual trajectories:

  This research applies a pairing process based on the prediction of merging potential. The pairing process can associate the mainline gaps with on-ramp vehicles. Thus, the mainline vehicles only open and keep gaps for on-ramp vehicles which are possible to merge without any additional controls naturally. Compared with those methods which unintendedly open gaps (e.g., Gap Metering), this proposed method has a smaller impact on the mainline traffic and has a more efficient utilization of mainline gaps.

- A vehicle-gap pair synchronization control algorithm:

  The control algorithm is basically derived from bi-directional cooperative adaptive cruise control. However, the target leading and lagging vehicles are not necessarily the physically surrounding vehicles but the paired putative sounding vehicles. This method guarantees the synchronization of the vehicle-gap pair starting from the upstream towards the merging location. The synchronization reduces waste of mainline gaps and makes the merging smoother and safer. Meanwhile, this method controls vehicles throughout the whole merging area. Thus, the mainline and on-ramp vehicles can gradually change their speed while approaching the predicted merging location and finally reach the desired merging speed. Unlike those methods which control vehicles' speed or acceleration onsite near a fixed merging

point, this method takes full utilization of acceleration lanes and lane capacity and reduces the impact of merging vehicles on other traffic.

- A multi-level pairing and control scenarios:

  The features of different vehicle type are considered in pairing and control stages. Different combination of vehicle types are classified in a 4-level merging scenario, and specific pairing criteria and control models are applied respectively. This method provides flexibility of the proposed method in the universal mixed vehicular environment.

- A VISSIM simulation-based performance evaluation:

  The proposed model is evaluated by a VISSIM simulation model calibrated with field data collected from the I-35 corridor in Austin, TX. The models and algorithms are implemented by VISSIM's external drivers' model. The traffic entry rate desired speed, and path split rate in the simulation is well configured to make the flow rates in mainline and ramp close to the observed field data. The model's performance is evaluated in both mobility and safety aspects. The simulation results show that the system can achieve a good balance between mobility and safety, especially it has an outstanding performance for on-ramp traffic in peak hours. In addition, the sensitivity analysis shows the system performance is improved along with the increase of market penetration rate of the C/AVs.

8.3 Implementation Recommendations

The proposed DMA system will be deployed in selected freeway merging sections where bottleneck congestions occur. Implementation and installation of the system will be

flexible. In the first stage of implementation, all devices will be installed on mobile infrastructures (i.e., vans or removable poles) which allow system adjustment based on local merging needs, environmental limits, and system performance. Then the system will be deployed to the locations where there're high system efficiency and stability with a permanent installation. The DMA system is a local and independent system that one system controls one merging section, and multiple DMA systems are not necessarily coordinating with each other despite the connection and coordination of multiple DMA systems in freeway network may benefit more.

8.3.1 System Components

The proposed DMA system has several modules and implements all steps of system function. The potential features of the proposed DMA system which will support the traffic management in freeway merging and weaving sections include:

- Data collection by sensor technologies

    o Environment data collection: Collect the road-network geometry information build the coordinates system.

    o Real-time traffic data collection: Collect the traffic information (e.g., vehicles' location and speed).

- Control the traffic in the target area

    o Vehicle trajectories processing and prediction: Estimate the instantaneous trajectories and potential merging location and timing of the vehicles whose location and speed are recorded.

o Create a DMA control strategy: Generate vehicle-gap pairing, mainline gap maintaining and onramp vehicle approaching control strategies.

- Control-Messages distribution

o V2I communication: The control signal will be delivered to vehicles through CV V2I communication.

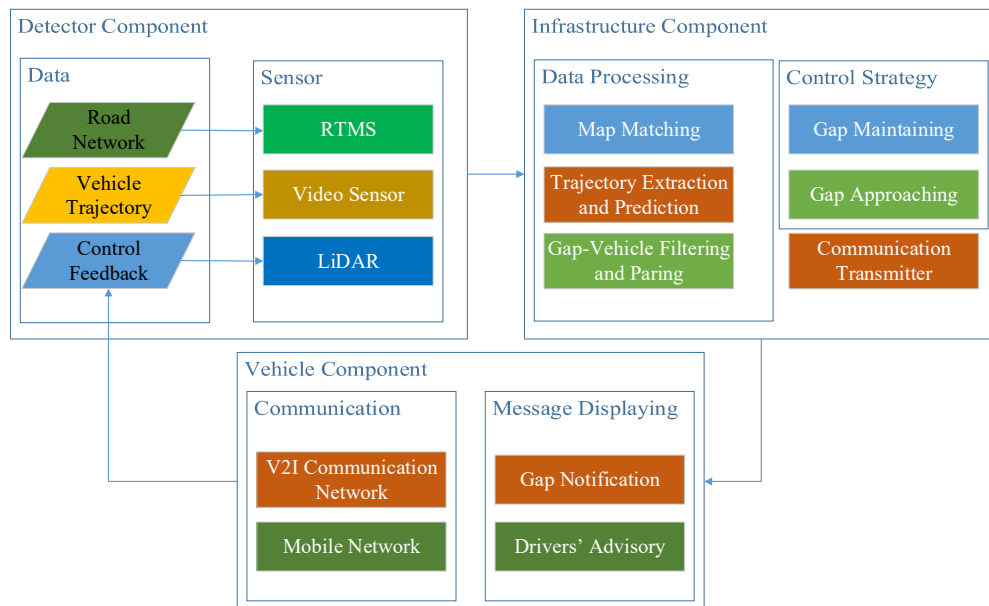o Control message display: The onboard unit will display the suggested speed.

Figure 23 DMA System Components

8.3.2 Required Devices

The system is designed as two major parts of devices: roadside-unit (RSU) and onboard-unit (OBU). Specifically, the roadside-unit includes sensing devices and control center while the onboard-unit is information display devices. In addition, the devices for a

communication network which connects the roadside-unit and onboard-unit is also necessary. The following are the detailed device requirement:

- Roadside-Unit

    o Roadside Sensors

    The required sensors include LiDAR sensor, high angle video camera, and RTMS sensor. The LiDAR sensor will be used to collect the geometry and background environment of the road network. The LiDAR devices can be equipped on a pole beside the target location, or on the top of a mobile van if the environment allows. Meanwhile, the high angle video camera will be used to capture the real-time traffic situation. RTMS sensor will be used as complementary to collect the real-time traffic volume and speed as well as the spacing between vehicles.

    o A computer workstation as the control center

    The control center will take charge of data processing and control strategies generation. A workstation with large storage and the fast processor is necessary.

    o Wireless Communication Station

    The communication station will be used to either build a local wireless network using DSRC technology or connect the local devices with public internet to distribute control message to drivers as well as receive the feedback and drivers' response.

- Onboard-Unit

o Communication Receiver

The communication receiver will be used to connect the onboard terminal with the local wireless network and/or the public Internet to get communication with the roadside infrastructures.

o Portable display devices

The control messages will be displayed on this device. It will be a smartphone APP or a programmed display device.

o Onboard Range Sensors

The onboard range sensors are primarily LiDAR, high definition radar, and/or cameras. The onboard range sensors are used to collect the location and speed of surrounding vehicles. The detection will be transmitted to the roadside unit to compose lane speed profiles.

8.3.3 System Operation

The operation of the proposed DMA system has three stages:

- System Installation: Install the required devices including sensors and control/communication stations.

In this step, the required devices will be installed for system deployment. The detector component and infrastructure component will be installed nearby the operation area as roadside-units while the vehicle component will be installed on users' vehicle. In addition, some of the equipped users' vehicles will also equip the

RTMS sensor within their vehicle component in order to detect the exact spacing between the preceding vehicle and itself.

- System Pre-Configuration: Generate the local High-definition map for vehicle positioning and tracking. Meanwhile, real traffic data will be collected for model calibration and update the parameters of the control model.

  o Environment information collection and rebuilding

  In this step, the environment information including road geometry, obstacles, and necessary surroundings will be scanned by the LiDAR sensor, and the obtained data points will be rebuilt as a 3-D model in the system.

  o Historical traffic data collection and model calibration

  In this step the historical traffic data including both the macroscopic ones such as volume rate, density, flow speed and the microscopic ones such as individual vehicles' speed, location, etc. The data will be used to calibrate the control model and to evaluate system performance.

- System Running: During the system running, the control signal will be distributed through CV V2I communication network. The delivered message includes gap notification and drive-advisory (i.e., speed advisory and lane change advisory).

  o Real-time traffic data collection and processing

During the DMA system running, real-time traffic information will be collected for trajectory generation and prediction. Based on the collected data, the system will generate control strategies and relevant control messages.

o Generate Control Strategies

The control objective is to conduct vehicle-level gap coordination and synchronization to ensure the effectiveness of the system.

o Control message distribution

The control messages will be distributed via a V2I communication network to the vehicles equipped with onboard receivers and display devices. The delivered message includes driving instruction for CAVs or gap notification and drive-advisory (i.e., speed advisory and lane change advisory) for CVs.

- The incentive of User Participant

Users can get mobility and safety benefit if they participate in the proposed DMA system, and the performance of the global traffic in the covered area will also be improved along with the increasing participants. These benefits are also critical for highway traffic management. However, the users will be more active to participate in the system if they can get some direct personal incentives. The possible incentives are:

o Direct Cash Bonus

Many car insurance companies provide programs which give the drivers a discount on insurance premium if they install a driving behavior recording

and analysis device onboard. The proposed system can possibly take a corporation with car insurance companies to provide similar incentive programs. The data collected by the system and the improvement of the highway system performance can be converted to the compensation for the insurance companies.

o   Driver Reputation and Credit

The proposed system can improve the overall performance of the whole traffic. It also can save energy and reduce pollution. Thus, the participated drivers can be considered as an eco-driver with a relatively higher reputation. The higher driving reputation can be awarded by a prize or lottery program, or even a discount in a gas station. Block-chain can be used to credit and record the driver behavior, which can combine the DMA system participant with other good driving behavior judgment system and energy-saving programs.

8.4 Suggested Future Work

Future work for this study includes the development of efficient calibration methods on the model parameters and the improvement on the accuracy and efficiency of IVT prediction and vehicle paring process. Other model-based performance measures will be explored to formulate efficient dynamic optimization models for model calibration. The pairing process in this work follows the "gap metering" strategy to guide gap opening and coordinate mainline and ramp traffic. Other dynamic merge and zipper merge strategy may be implemented to improve its performance further.

Reference

Antoniotti, M., Desphande, A., & Girault, A. (1997). *Microsimulation analysis of multiple merge junctions under autonomous ahs operation.* Paper presented at the Intelligent Transportation System, 1997. ITSC'97., IEEE Conference on.

Bauer, C. S., & Risher, T. A. (1977). *Simulation Analysis of A Computer-Controlled Freeway Merging System.* Paper presented at the IEEE Tech Digest Vehicular Tech Group Conf.

Buhr, J. H., Radke, M., Kirk, B., & Drew, D. (1969). A moving vehicle merging control system.

Bushnell, D. (1970). A merging control system for the urban freeway. *Vehicular Technology, IEEE Transactions on, 19*(1), 107-120.

Choi, S.-T., Hur, W.-S., & Seo, S.-W. (2014). *Cooperative localization based on topology matching.* Paper presented at the Wireless Vehicular Communications (WiVeC), 2014 IEEE 6th International Symposium on.

Datta, T. K., Schattler, K. L., Kar, P., & Guha, A. (2004). Development and Evaluation of an advanced dynamic lane merge traffic control system for 3 to 2 lane transition areas in work zones.

Davis, L. (2007). Effect of adaptive cruise control systems on mixed traffic flow near an on-ramp. *Physica A: Statistical Mechanics and its Applications, 379*(1), 274-290.

Fujii, S., Fujita, A., Umedu, T., Kaneda, S., Yamaguchi, H., Higashino, T., & Takai, M. (2011). *Cooperative vehicle positioning via V2V communications and onboard sensors.* Paper presented at the Vehicular Technology Conference (VTC Fall), 2011 IEEE.

Fujita, A., Yamaguchi, H., Higashino, T., & Takai, M. (2016). *A study on identification of laser-tracked vehicles using V2V-based velocity information.* Paper presented at the 2016 IEEE 17th International Symposium on.

Gipps, P. G. (1981). A behavioural car-following model for computer simulation. *Transportation Research Part B: Methodological, 15*(2), 105-111.

Grillo, L., Datta, T., & Hartner, C. (2008). Dynamic late lane merge system at freeway construction work zones. *Transportation Research Record: Journal of the Transportation Research Board*(2055), 3-10.

Hall, R. W., & Tsao, H. J. (1997). *Capacity of automated highway systems: merging efficiency.* Paper presented at the American Control Conference, 1997. Proceedings of the 1997.

Hayat, M. T., Park, H., & Smith, B. L. (2014). *Connected vehicle enabled freeway merge assistance system-field test: preliminary results of driver compliance to advisory.* Paper presented at the Intelligent Vehicles Symposium Proceedings, 2014 IEEE.

Hedrick, J., Tomizuka, M., & Varaiya, P. (1994). Control issues in automated highway systems. *Control Systems, IEEE, 14*(6), 21-32.

Hellernan, B. (June 8, 2010). Managed Motorways in the Netherlands. *Centre for Transport and Navigation, Presentation to the FGD Scan Team.*

Jiang, X., Jin, P. J., Wan, X., & Wang, Y. (2017). A V2I (Vehicle-to-Infrastructure) based Dynamic Merge Assistance Method based on Instantaneous Virtual Trajectories: A Microscopic Implementation of Gap Metering.

Jin, P. J., Fang, J., Jiang, X., DeGaspari, M., & Walton, C. M. (2016). Gap Metering for Active Traffic Control at Freeway Merging Sections. *Journal of Intelligent Transportation Systems*, 00-00. doi: 10.1080/15472450.2016.1157021

Jin, P. J., Fang, J., Jiang, X., DeGaspari, M., & Walton, C. M. (2017). Gap metering for active traffic control at freeway merging sections. *Journal of Intelligent Transportation Systems, 21*(1), 1-11.

Jin, P. J., Yang, D., & Ran, B. (2014). Reducing the error accumulation in car-following models calibrated with vehicle trajectory data. *Intelligent Transportation Systems, IEEE Transactions on, 15*(1), 148-157.

Kachroo, P., & Li, Z. (1997). *Vehicle merging control design for an automated highway system.* Paper presented at the Intelligent Transportation System, 1997. ITSC'97., IEEE Conference on.

Kang, K.-P., Chang, G.-L., & Paracha, J. (2006). Dynamic late merge control at highway work zones: evaluations, observations, and suggestions. *Transportation Research Record: Journal of the Transportation Research Board*(1948), 86-95.

Klee, H. (1973). An Algorithm for Synchronizing Entrance Ramp Vehicles and Freeway Gaps. *Journal of Dynamic Systems, Measurement, and Control, 95*(2), 204-212.

Letter, C., & Elefteriadou, L. (2017). Efficient control of fully automated connected vehicles at freeway merge segments. *Transportation Research Part C: Emerging Technologies, 80*(Supplement C), 190-205. doi: https://doi.org/10.1016/j.trc.2017.04.015

Lu, X.-Y., Tan, H.-S., Shladover, S. E., & Hedrick, J. K. (2004). Automated vehicle merging maneuver implementation for AHS. *Vehicle System Dynamics, 41*(2), 85-107.

Margiotta, R. A., Spiller, N. C., & Halkias, J. A. (2007). Traffic Bottlenecks: A Primer–Focus on Low-Cost Operational Improvements.

Marinescu, D., Čurn, J., Bouroche, M., & Cahill, V. (2012). *On-ramp traffic merging using cooperative intelligent vehicles: A slot-based approach.* Paper presented at the Intelligent Transportation Systems (ITSC), 2012 15th International IEEE Conference on.

Marinescu, D., Čurn, J., Slot, M., Bouroche, M., & Cahill, V. (2010). *An active approach to guaranteed arrival times based on traffic shaping.* Paper presented at the Intelligent Transportation Systems (ITSC), 2010 13th International IEEE Conference on.

Meyer, E. (2004a). Construction area late merge (CALM) system. *Technology Evaluation Report. Midwest Smart Work Zone Deployment Initiative. FHWA Pooled Fund study*.

Meyer, E. (2004b). Construction area late merge (CALM) system. *Kansas Department of Transportation*.

Milanés, V., Godoy, J., Villagrá, J., & Pérez, J. (2011). Automated on-ramp merging system for congested traffic situations. *IEEE Transactions on Intelligent Transportation Systems, 12*(2), 500-508.

Miller, M., Misener, J., Godbole, D., & Deshpande, A. (1999). Development of hierarchical methodology for benefit evaluation of vehicle-highway automation: Case study of the Houston Katy Freeway. *Transportation Research Record: Journal of the Transportation Research Board*(1679), 139-147.

Park, H., Bhamidipati, C., & Smith, B. (2011). Development and evaluation of enhanced intellidrive-enabled lane changing advisory algorithm to address freeway merge conflict. *Transportation Research Record: Journal of the Transportation Research Board*(2243), 146-157.

Park, H., Su, S., Hayat, M. T., & Smith, B. L. (2014). *A Prototype Freeway Merging Control Algorithm Under a Connected Vehicle Environment*. Paper presented at the Transportation Research Board 93rd Annual Meeting.

Pesti, G., & McCoy, P. (2001). Long-term effectiveness of speed monitoring displays in work zones on rural interstate highways. *Transportation Research Record: Journal of the Transportation Research Board*(1754), 21-30.

Pesti, G., Wiles, P., Cheu, R. L., Songchitruksa, P., Shelton, J., & Cooner, S. (2007). Traffic control strategies for congested freeways and work zones. *FHWA/TX Report, 8*, 0-5326.

Pesti, G., Wiles, P., Cheu, R. L., Songchitruksa, P., Shelton, J., & Cooner, S. (2008). Traffic control strategies for congested freeways and work zones: Texas Transportation Institute, Texas A & M University System.

Piotrowicz, G., & Robinson, J. (1995). Ramp Metering Status in North America. 1995 Update.

Ran, B., Leight, S., & Chang, B. (1999). A microscopic simulation model for merging control on a dedicated-lane automated highway system. *Transportation Research Part C: Emerging Technologies, 7*(6), 369-388.

Rauch, A., Maier, S., Klanner, F., & Dietmayer, K. (2013). *Inter-vehicle object association for cooperative perception systems*. Paper presented at the Intelligent Transportation Systems-(ITSC), 2013 16th International IEEE Conference on.

Rios-Torres, J., & Malikopoulos, A. A. (2017a). Automated and cooperative vehicle merging at highway on-ramps. *IEEE Transactions on Intelligent Transportation Systems, 18*(4), 780-789.

Rios-Torres, J., & Malikopoulos, A. A. (2017b). A survey on the coordination of connected and automated vehicles at intersections and merging at highway on-ramps. *IEEE Transactions on Intelligent Transportation Systems, 18*(5), 1066-1077.

Rohani, M., Gingras, D., & Gruyer, D. (2014, 3-7 Nov. 2014). *Vehicular cooperative map matching*. Paper presented at the 2014 International Conference on Connected Vehicles and Expo (ICCVE).

Saiprasert, C., & Thajchayapong, S. (2015). Remote Driver Identification Using Minimal Sensory Data. *19*(10), 1706-1709.

Sakr, A. H., & Bansal, G. (2016). *Cooperative localization via DSRC and multi-sensor multi-target track association*. Paper presented at the Intelligent Transportation Systems (ITSC), 2016 IEEE 19th International Conference on.

Scarinci, R., & Heydecker, B. (2014). Control concepts for facilitating motorway on-ramp merging using intelligent vehicles. *Transport reviews, 34*(6), 775-797.

Scarinci, R., Heydecker, B., & Hegyi, A. (2015). Analysis of traffic performance of a merging assistant strategy using cooperative vehicles. *IEEE Transactions on Intelligent Transportation Systems, 16*(4), 2094-2103.

Statista. (2017). Statista connected vehicle penetration rate in U.S., 2017, from https://www.statista.com/outlook/320/109/connected-car/united-states#

TAMU-TTI. (2015). 2015 Annual Urban Mobility Scorecard — Urban Mobility Information. from http://mobility.tamu.edu/ums/

Tignor, S. C. (1975). Operational analyses of freeway moving-merge systems. *Transportation research record, 533*, 1-21.

. Traffic Congestion and Reliability: Trends and Advanced Strategies for Congestion Mitigation. (2005). FHWA: Cambridge Systematics, Inc., Texas Transportation Institute.

True, J., & Rosen, D. (1973). MOVING MERGE--A NEW CONCEPT IN RAMP CONTROL. *Public Roads, 37*(7).

Xie, Y., Zhang, H., Gartner, N. H., & Arsava, T. (2017). Collaborative merging strategy for freeway ramp operations in a connected and autonomous vehicles environment. *Journal of Intelligent Transportation Systems, 21*(2), 136-147.

Yuan, T., Krishnan, K., Chen, Q., Breu, J., Roth, T. B., Duraisamy, B., . . . Gern, A. (2017). Object matching for inter-vehicle communication systems—An IMM-based track association approach with sequential multiple hypothesis test. *18*(12), 3501-3512.

Yuan, T., Krishnan, K., Duraisamy, B., Maile, M., & Schwarz, T. (2017). *Extended object tracking using IMM approach for a real-world vehicle sensor fusion system.* Paper presented at the Multisensor Fusion and Integration for Intelligent Systems (MFI), 2017 IEEE International Conference on.

Zhou, M., Qu, X., & Jin, S. (2017). On the impact of cooperative autonomous vehicles in improving freeway merging: a modified intelligent driver model-based approach. *IEEE Transactions on Intelligent Transportation Systems, 18*(6), 1422-1428.